Ab initio density-functional supercell calculations of hydrogen defects in cubic SiC

B. Aradi
Department of Atomic Physics, Budapest University of Technology and Economy, Budafoki út 8, H-1111, Budapest, Hungary

A. Gali
Research Group of the Hungarian Academy of Sciences, H-1521, Budapest, Hungary

P. Deák
Department of Atomic Physics, Budapest University of Technology and Economy, Budafoki út 8, H-1111, Budapest, Hungary

J. E. Lowther
Department of Physics, University of the Witwatersrand, P. O. Box 2050, Johannesburg, South Africa

N. T. Son and E. Janzén
Department of Physics and Measurement Technology, University of Linköping, Linköping, S-58183, Sweden

W. J. Choyke
Department of Physics and Astronomy, University of Pittsburgh, Pittsburgh, Pennsylvania 15260
(Received 11 December 2000; published 29 May 2001)

Based on *ab initio* density-functional calculations in supercells of 3*C*-SiC, the stable configurations of hydrogen and dihydrogen defects have been established. The calculated formation energies are used to give semiquantitative estimates for the concentration of hydrogen in SiC after chemical vapor deposition, low temperature H-plasma anneal, or heat treatment in high temperature hydrogen gas. Vibration frequencies, spin distributions, and occupation levels were also calculated in order to facilitate spectroscopic identification of these defects. ($V+n$H) complexes are suggested as the origin of some of the signals assigned earlier to pure vacancies. Qualitative extrapolation of our results to hexagonal polytypes explains observed electrical passivation effects of hydrogen.

DOI: 10.1103/PhysRevB.63.245202 PACS number(s): 71.15.Mb, 71.55.Ht, 61.72.Bb, 61.72.Ji

I. INTRODUCTION

Hydrogen is one of the most common impurities in semiconductors, introduced by both wet and dry etching among other methods. Due to its profound and very varied influence on the electronic characteristics of the material (passivation of electrically active centers, formation of large active complexes), interest in theoretical and experimental research on the hydrogen impurity in semiconductors has been continuous in recent years.[1–3] Silicon carbide (SiC) is a wide band gap semiconductor that has been known for a very long time, but its technology is just reaching maturity for practical application in power electronic devices. The data base necessary for defect engineering is still in the making for this material. The present paper tries to contribute to this process with results of first-principles model calculations on hydrogen-related defects. Hydrogen has a special importance for SiC: due to the difficulties with bulk crystal growth and diffusion doping, in-growth-doped homoepitaxial layers prepared by chemical vapor deposition (CVD) from hydrogen-rich precursor molecules play a crucial role in devices. Hydrogen is therefore a natural contaminant of such layers. Since doping utilizes the competition of dopants and host atoms for a given site in the crystal,[4] hydrogen competing for the free valences of a vacancy may influence doping efficiencies.[5] That—together with the expected passivation effect of hydrogen on radiation induced defects—makes vacancy + hydrogen complexes a primary target for investigation. Naturally, the energetics and kinetics of hydrogen related defect complexes (whether with intrinsic or with extrinsic defects) cannot be established without knowing the energies of the stable configurations of interstitial hydrogen in various charge states, as well as the energies of dihydrogen complexes. In this study the interaction of one or two hydrogen atoms is considered with the ''perfect'' lattice and with an isolated vacancy (at both the C and the Si sites) in SiC.

As in other semiconductors, passivation of shallow donors and acceptors due to hydrogen is expected in SiC as well. Except for boron-doped 6*H*-SiC samples, where it was shown with SIMS (secondary ion mass spectrometry) and PL (photoluminescence spectroscopy),[5,6] very little is known about hydrogen incorporation during epitaxial growth. Those samples showed strong decrease in carrier concentration due to hydrogen. Annealing wafers cut from boules of 6*H*-SiC in H_2 atmosphere between 1500 and 1700 °C resulted in 90% loss in carrier concentration in *p*-type samples moderately doped with Al ($[p]\sim 10^{17}$ cm^{-3}), and 75% loss in *n*-type samples heavily doped with N ($[n]\sim 10^{19}$ cm^{-3}),[7] but no H-related vibrations were found in either case.[8] Hydrogen-plasma anneal of *p*-type 4*H*-SiC epilayers (doped with Al to $[p]\sim 10^{18}$ cm^{-3}) at low temperature (250 °C) also caused a decrease in the free carrier concentration.[9] Since a postanneal at 500 °C caused further decrease, passivation due to dopant-

hydrogen complex formation seemed more likely than carrier trapping in defects created by the plasma. At a doping level of 7×10^{17} cm^{-3}, the passivation was much more prevalent in *p*-type than in *n*-type samples in a 300 °C electron cyclotron resonance plasma, and a heat treatment around 700 °C was needed for reactivation.[10] Low energy implantation of $^2H_2^+$ into lightly doped *p*-type [$(5-10)\times10^{15}$ cm^{-3}] 4*H* epilayers passivated or at least compensated B completely and Al to a large extent, but no passivation and little incorporation (at room temperature, none at 400 °C) was found in the case of samples doped at the same level [$(5-10)\times10^{15}$ cm^{-3}] with N.[11] The passivation of Al occurred by complex formation. The Al-H complex could be dissociated by ~1.8 eV, and released hydrogen in the positive charge state.[12] A substantial decrease of the free carrier concentration after H implantation into heavily doped *n*-type ($\sim10^{19}$) 4*H*-SiC was reported based on spectroscopic ellipsometry studies.[13] However, the passivation was attributed to electron traps created during implantation. This effect was also demonstrated in dc plasma treatment of N-doped [$(0.2-3)\times10^{18}$ cm^{-3}] samples between 300 and 700 °C.[14]

In summary, H appears to be easily incorporated into *p*-type samples where it may cause passivation, or at least compensation of dopants. Except for high temperature, high pressure annealing in H_2, hydrogen enters *n*-type samples less easily. The effect of H-plasma treatment of or H implantation into *n*-type samples is the creation of electron traps.

Apart from passivation studies, very few papers have been published on H in SiC, and the experimental fingerprints of its main forms have not yet been established. Photoluminescence bands arising as phonon replicas due to local modes at 2962, 2977, and 2988 cm^{-1} in 6*H*- and 2959 and 2985 cm^{-1} in 4*H*-SiC after H^+ implantation of *p*-type material grown in a C-rich environment were interpreted as C-H stretch modes due to H in silicon vacancies at different inequivalent sites.[15,16] Vibrations that could be assigned to Si-H stretching modes ($\sim$2100 cm^{-1}) have not yet been observed. Diffusion of H in lightly doped 6*H*- and 4*H*-SiC after implantation at 50 keV (10^{15} cm^{-2}) has been investigated.[17,18] In these works a dissociation energy between 3.5 and 4.9 eV was estimated as the rate limiting step, assuming that hydrogen decorates silicon vacancies. It was found that hydrogen diffuses considerably more slowly in *n*-type than in *p*-type samples.[19] No DLTS (deep level transient spectroscopy) peaks could be related to hydrogen in electron-irradiated and deuterium-implanted 6*H*-SiC.[20] As yet no EPR (electron paramagnetic resonance) signals related to H have been observed either, but muon spin resonance (μSR) experiments indicate muonium (an analog of the H atom made of a muon and an electron) to be at tetrahedral interstitial sites (see Ref. 21 and references therein). This general lack of information about H in SiC (especially in epilayers) is intriguing, so *a priori* knowledge about its various forms and about the conditions under which they are formed could be helpful—even if the data supplied by model calculations are only approximate.

The only theoretical studies we are aware of in SiC considered hydrogen solely as an isolated interstitial in the neutral charge state, using a molecular cluster model.[22,23] The equilibrium position of H^0 in 3*C*-SiC was found at the tetrahedral interstitial site in the cage of the less electronegative atoms Si (at T_{Si}). This result is similar to the one found in GaAs,[24] and for a number of other binary semiconductors.[22] In contrast, the most stable position of H^0 in diamond[25] and silicon[26–28] is the bond-center (BC) site, i.e., hydrogen interrupts a bond between two host atoms, forming a *three-center bond*. Two electrons in a state formed by the symmetric combination of the sp^3 hybrids of two neighboring host atoms and of the *s* orbital of the hydrogen envelop all three atoms.

The technologically important silicon carbide polytypes are the hexagonal 4*H*-SiC and 6*H*-SiC (with *ABAC* and *ABCACB* stacking sequences of Si-C atomic double layers along the [0001] direction, respectively). These can be grown as bulk single crystals of electronic quality. For cubic (zinc-blende) 3*C*-SiC (with an *ABC* stacking sequence along the [111] direction) this has not yet been achieved, but this is the preferred polytype in heteroepitaxy on large silicon wafers (still far from electronic quality). The 3*C* polytype has the smallest unit cell while that of 4*H* (6*H*) is four (six) times bigger. Since the computational cost for our method scales with the third power of size, it is reasonable to do large scale exploratory calculations on 3*C*-SiC first. The first- and second-neighbor environment is the same in all polytypes, but the band gap of 3*C*-SiC (2.4 eV) is significantly smaller than that of 4*H*-SiC (3.3 eV) or 6*H*-SiC (3.0 eV). With proper caution, however, it is possible to give at least qualitative estimates of the behavior of defects in the hexagonal polytypes, based on calculations in the cubic one.

Our paper is organized as follows. In Sec. II we describe the theoretical methods we use to study one- and two-hydrogen defects in intrinsic 3*C*-SiC. Results will be given in Sec. III. Sec. III A contains the results on atomic interstitial hydrogen in all three charge states, while Sec. III B is about interstitial dihydrogen complexes. In Sec. III C we report on one or two hydrogen atoms in a silicon vacancy. Results published recently[29] on hydrogen in the carbon vacancy will also be reiterated briefly in Sec. III D. Finally, we establish the relative stability of the different complexes in Sec. III D. Based on that and on the calculated electronic and vibronic properties we comment on the passivating capabilities of hydrogen and discuss experimental information (or the lack thereof) about H in SiC in Sec. IV. Some of the results mentioned here have been published in a preliminary form.[30]

II. METHOD

First-principles calculations using the local density approximation (LDA) to density-functional theory[31] were carried out in a supercell model (SCM) of the defective solid. To explore relative stabilities of different configurations, a 32-atom (bcc) unit cell was used. The most stable configurations of the individual defect in each charge state were recalculated in a 128-atom (fcc) unit to obtain formation energies and occupation levels, as well as one-electron wave functions. For these computations, the FHI98MD code[32] was

TABLE I. Comparison of the formation energies of various defects under stoichiometric conditions as obtained from the 32- and 128-atom SCM calculations (present work). No LDA gap correction and zero point energy are added in order to make comparison with the results of Ref. 38 possible. μ_H is the chemical potential of H.

Defect	E^q_{form} (eV)		
	32-atom SCM	128-atom SCM	216-atom SCM
V_C^0	4.89	4.49	4.30
$(V_C+H)^0$	$-10.57-\mu_H$	$-10.76-\mu_H$	
$(V_C+2H)^0$	$2\times(-12.94-\mu_H)$	$2\times(-12.98-\mu_H)$	
V_{Si}^0	8.66	8.16	8.45
$(V_{Si}+H)^0$	$-9.11-\mu_H$	$-9.36-\mu_H$	
$(V_{Si}+2H)^0$	$2\times(-13.19-\mu_H)$	$2\times(-13.16-\mu_H)$	
$(H_2)_{T_{Si}}$	$2\times(-13.72-\mu_H)$	$2\times(-13.59-\mu_H)$	
$H^0_{AB_C}$	$-13.48-\mu_H$	$-13.23-\mu_H$	

[a]Reference 38.

applied, which utilizes a plane wave basis. In the 32-atom calculations a high kinetic energy cutoff of 64 Ry was used with Troullier-Martins norm-conserving soft-core pseudopotentials.[33] This makes both perfect crystal and relative defect energies converged within 0.01 eV. For the 128-atom calculations the cutoff was reduced to 32 Ry, with a simultaneous adjustment of the core radii in the pseudopotential. The energy convergence is still better than 0.05 eV.[34] The LDA is known to underestimate the width of the gap. While the experimentally observed excitation energies can be reproduced with a more or less rigid shift of the energies of extended states in the conduction band (with respect to the edge of the valence band), defect orbitals, which are mixtures of valence and conduction band states, represent a problem. Therefore, defect levels in the gap have been shifted proportionally to their overlap with the conduction band (CB) states.[35] The total energy was then corrected by this shift times the occupation number of the defect state. Summation over the reduced Brillouin zone of the supercells was carried out using the $2\times2\times2$ Monkhorst-Pack (MP) scheme[36] for both the 32- and 128-atom units. It has to be noted that in the case of the zinc-blende lattice these sets do not include the critical **k** points at (near) the band edges; therefore the ''gap'' between the explicitly treated occupied and unoccupied one-electron energies is substantially higher than the LDA minimum gap. This situation is advantageous in avoiding artificial occupation of the CB edge instead of a localized defect level because of the LDA gap error (which is corrected only *a posteriori*). If the defect level turned out to be higher in energy than the corrected position of the CB edge, the calculation was repeated with a $3\times3\times3$ MP set, which includes the necessary band edge states. Another correction in the position of defect levels and total energy is made necessary by the dispersion due to the interaction of repeated defects in the SCM. An approximate position of the ''isolated'' defect level was found by fitting a tight binding dispersion relation to the energies calculated at different **k** points.[37] The total energy was then corrected by the differences between this value and the defect levels calculated at the individual **k** points (times the occupation number). An additional source of inaccuracy in the relative stabilities arises because of the limitations of our code to spin-unpolarized calculations. (The energies of isolated atoms in vacuum were, however, determined with spin polarization.) In the case of the vacancies the error of neglecting spin polarization is known from the work of Zywietz *et al.*[38,39] We will assume that for $(V+H)$ and $(V+2H)$ defects the error is roughly the same. So the energies of doublet, triplet, and quadruplet states were corrected with $-0.1,-0.2$, and -0.5 eV, respectively.[40] In the case of interstitial H, we will use the data obtained for the silicon crystal, where the spin polarization error for H at the tetrahedral interstitial site was -0.1 eV and at the bond-center site -0.02 eV.[41]

The total energy of the perfect SCM was minimized with respect to the Si-C distance, and the latter was found to be within 0.8% of the experimental value. The geometry of minimum energy for the defects is found by allowing two shells of host atom neighbors to relax and reconstruct with or without symmetry constraints in the 32-atom SCM. The convergence criterion for the forces was 0.0005 hartree/bohr. Tests with third-neighbor relaxation in the 128-atom SCM showed that for the defects under consideration this restriction does not cause significant error. Therefore, defect calculations in the 128-atom unit were carried out at the optimum geometry found in the 32-atom calculation. As a consequence, the formation energies are upper bounds for neutral defects.[42] We expect the accuracy of the $(+/0)$ and $(0/-)$ occupation levels to be within about ±0.15 eV. (In the case of the occupancy level between higher charge states the error may be larger.) Convergence of the results can be checked in Table I, where formation energies obtained from the 32- and from the 128-atom units are compared. In the case of the vacancies, our results can also be compared to those of Ref. 38 obtained from a 216-atom SCM with a $4\times4\times4$ MP set (but with a different type of pseudopotential and corresponding cutoff). The uncorrected occupation levels obtained for the vacancies in this work also match within 0.1 eV with those of Ref. 39.

Prediction of the local vibrational mode (LVM) frequencies by theory is of special importance in the experimental identification of defect centers. Calculating vibrational fre-

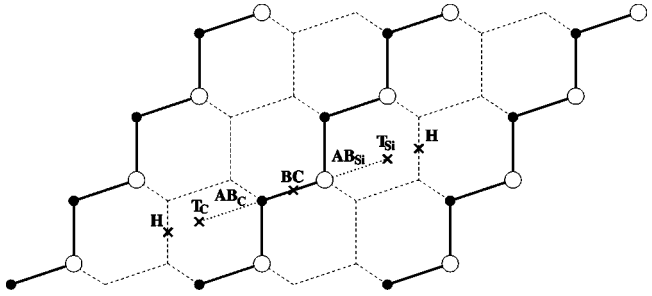

FIG. 1. Interstitial sites in the (110) plane of 3*C*-SiC. Black and white circles represent C and Si atoms, respectively.

quencies on a plane wave basis with a high energy cutoff is very time consuming. However, the interatomic forces are predominantly determined by the valence electrons of the crystal and the localized electrons of the defect. Therefore, frequencies were calculated using a supercell version of the AIMPRO code,[43] which applies the LDA on a localized basis of uncontracted Gaussian-type orbitals (with preoptimized exponents) in conjunction with norm-conserving nonlocal Bachelet-Hamann-Schlüter pseudopotentials.[44] A basis with four *s*-type and four *p*-type Gaussians was used for each Si or C atom while two *s* and two *p* Gaussians were included for hydrogen atoms. In addition an *s*-type Gaussian was put at each bond center to simulate polarization functions. For these calculations a 64-atom (sc) unit cell was used with the $\mathbf{k}=\mathbf{0}$ approximation. Geometries obtained from the plane wave calculations were refined under identical constraints (no significant change was observed in all but one case). The LVM frequencies were obtained in the harmonic approximation by calculating the second derivatives of the total energy with respect to all relaxing atoms. Local modes were selected based on the amplitudes of the atoms. The frequencies of stretching mode vibrations distinct from the continuum of SiC vibrations are typically[45] accurate within about 50 cm^{-1}, but differences (like isotope shifts) are reproduced within a few wave numbers.

III. RESULTS

A. Interstitial atomic hydrogen

Based on experience with other semiconductors, the equilibrium position of a neutral interstitial hydrogen atom (H^0) was sought in the 32-atom unit by starting symmetry unrestricted geometry optimizations with H^0 near the T_{Si}, T_C, and BC sites. (The important sites of the 3*C*-SiC lattice can be seen in Fig. 1.) Three local minima have been found. H^0 is most stable 0.69 Å away from T_C along [111], in an AB_C position. It forms a bond ($d_{H\text{-}C}=1.14$ Å) with the nearest C neighbor and the C-Si bond further along that direction is weakened ($d_{C\text{-}Si}=1.95$ Å). In fact, it would be more appropriate to speak of a three-center bond on the H-C-Si unit. One metastable configuration was found 0.08 Å away from the T_{Si} site along [111] (nearer to the Si atom). This configuration is 0.66 (0.58) eV less stable in the 32- (128-)atom calculation than the AB_C site (neglecting differences in zero point energy). The nearest Si-C bond remains almost unperturbed. The electronic structure is almost identical with that found at T_{Si}, which is not a minimum in energy. H at the BC site is also metastable, 0.62 eV higher in energy than at AB_C.

Our result contradicts that of the molecular cluster model (MCM) calculation of Ref. 23, where the most stable site was found to be T_{Si}. In a test calculation using the AIMPRO code on a MCM similar to that of Ref. 23, we also get H^0 near T_{Si} to be significantly more stable than on the AB_C site, while the AIMPRO calculation on a 64-atom SCM gave the same results as the FHI98MD code on the 32-atom SCM. The reason lies in the inadequate description of the delocalized conduction band states in a MCM calculation, leading to a very wide gap in the electronic structure of the cluster. As a consequence, a state localized strongly to hydrogen appears within this gap with H at either the T_{Si} or the T_C site. The electron in this orbital is in an area of low electron density in the former and in a higher density one in the latter case. As a result, both the one-electron level and the total energy are lower for H^0 at T_{Si}. In the SCM calculation the aforementioned localized level is still in the gap for H at T_{Si}; however, at T_C it lies well above the (corrected) CB edge. (All the one-electron levels are displayed together in Fig. 2.) As a result, in the latter case, the electron of H^0 occupies a delocalized state nearly identical with the lowest conduction band state of the perfect supercell. The three-center bond with the C-Si unit is formed, offsetting the energy advantage of the one-electron state in the nonbonded H^0 at T_{Si}. With H in the AB_C configuration, an orbital largely localized on H (essentially the ''antibonding'' counterpart of the localized three-center bond) lies more than 1 eV above the CB edge. Since the gap of the 6*H* and 4*H* polytypes is wider by only

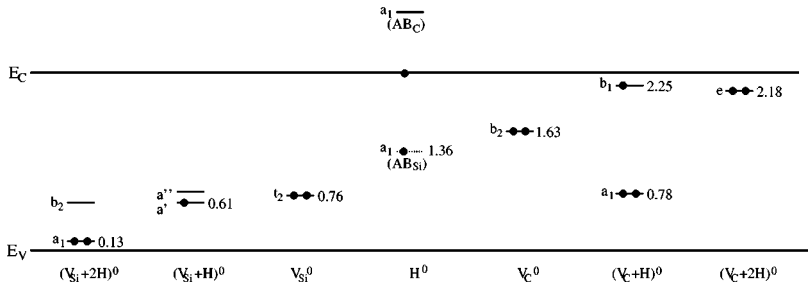

FIG. 2. The calculated one-electron levels for various defects in 3*C*-SiC in the neutral charge state. The energies in eV of the one-electron levels are given with respect to the valence band. (In the charged states the one-electron levels are shifted compared to their positions in the neutral states).

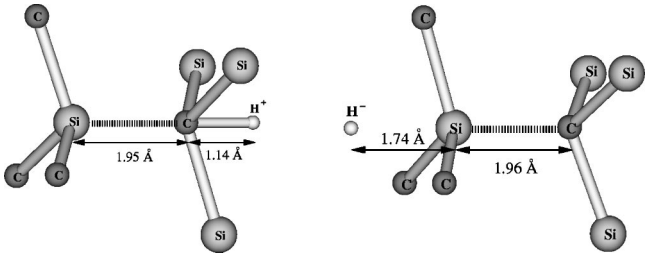

FIG. 3. The geometry of the charged states of interstitial atomic H in 3*C*-SiC.

0.6 and 0.9 eV, respectively, we expect a similar bonding situation at an AB_C site there too. However, the larger gap will increase the energy of this configuration with respect to H at T_{Si}. Therefore, in the hexagonal polytypes the latter is likely to be energetically favorable as predicted in Ref. 23.

Changing the charge state we find that H^+ prefers the AB_C and H^- the near to T_{Si} position (Fig. 3), by 0.7 eV over the BC site in the former case and by 1.3 eV over T_C in the latter (both values refer to 32-atom calculations without zero point energy). Considering the $-(+)$ charge on C (Si) in the host lattice, this situation is expected intuitively. It has to be noted, though, that in the positively charged case the (Si-)C-H bond is essentially a covalent three-center bond, and the ionization has occurred from the delocalized CB state. (The geometry is essentially identical with that of the neutral charge state.) In the negative charge state only about half of the extra charge is localized on hydrogen and the rest weakens the Si-C bond. The ionized one-electron state begins to resemble the ''antibond'' of a weak (H-)Si-C three-center bond.

The relative stabilities of the three charge states as a function of the Fermi level position are shown in Fig. 4 as obtained from the 128-atom calculations. H^0 appears to have a stability window of ~ 0.1 eV, but considering the uncertainties of the calculation a negative *U* behavior (the charged states being always more stable than the neutral state) cannot be excluded. The $(+/0)$ occupation level is at $E_V + 2.32$ eV, while the $(0/-)$ occupation level at $E_V + 2.405$ eV is almost degenerate with the CB edge. So interstitial H may act as a relatively shallow donor in 3*C*-SiC. Because of their localized nature, we do not expect the energies of the charged states to change dramatically in the hexagonal polytypes. However, as explained above, the total energy of the neutral state may increase. This could lead to negative *U* behavior with a $(+/-)$ occupation level around $E_V + 2.4$ eV in 4*H*- and 6*H*-SiC, making interstitial atomic hydrogen a deep electron *and* hole trap.

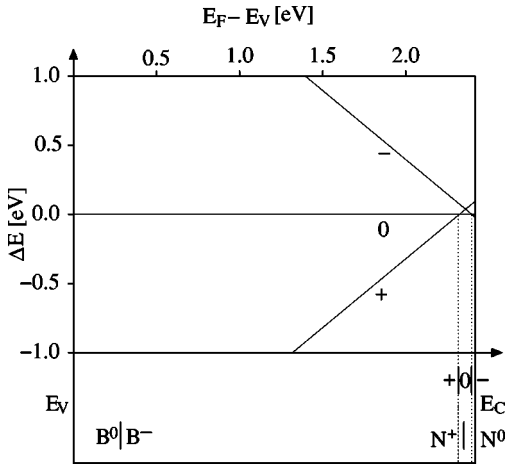

FIG. 4. Stabilitiy of the charge states of interstitial atomic H with respect to the neutral state in 3*C*-SiC as a function of the Fermi level position in the gap. The lower part of the figure shows the position of the occupation levels in the gap, compared with the occupation levels of the shallow dopants.

With the narrow stability window we obtain, H^0 or muonium (Mu) is not likely to be easily detectable by electron or muon spin resonance in equilibrium in 3*C*-SiC. It is, however, questionable whether μSR records equilibrium conditions. In fact, an isotropic μSR signal has been observed in 3*C*-SiC (see the review of Estreicher[21]). About 30% of the incoming muons take on this paramagnetic state, while the rest remains diamagnetic. Our prediction of the AB_C site implies a hyperfine interaction with axial symmetry. Of course, H^0 or Mu may occupy any of the four AB_C sites around T_C. We have calculated the approximate barrier between these sites along the [001] axis. Comparing its value of 0.47 eV with the zero point energy of Mu, 0.81 eV, it follows that an isotropic μSR signal will arise due to motional averaging even at very low temperatures. The same reasoning requires high temperature for H^0 which has a zero point energy of 0.27 eV.

The calculated stretch mode vibration frequency of H^+ in the (Si-)C-H bond at AB_C is 2747 cm^{-1}, somewhat lower than typical C-H frequencies. The reason is the slight ''overcoordination'' of the carbon atom.

B. Diatomic interstitial hydrogen

Stable dihydrogen complexes were sought by starting with two H atoms on different *AB* sites in a 32-atom unit. As in Si, the H_2 molecule at the T_{Si} site turns out to be the most stable dihydrogen complex. (H_2 at the T_C site is less stable by 1.94 eV.) The H_2 molecule can rotate almost freely around its center of mass. The [111] orientation is preferred but the energy difference with respect to the [001] orientation is less than 0.1 eV. The length of the H-H bond is 0.802 Å, to be compared to 0.779 Å calculated for the H_2 molecule in vacuum. The H-H stretching mode frequencies calculated in the harmonic approximation are 3452 cm^{-1} in the solid and 4227 cm^{-1} for the free molecule. $(H_2)_{T_{Si}}$ is more stable than two $(H^0)_{AB_C}$ by 1.70 (1.97) eV in the 32-(128-)atom calculation. For most Fermi level positions, H^0 is not stable in equilibrium in 3*C*-SiC. Therefore, the stability of H_2 relative to isolated interstitials will depend on the position of the Fermi level. As will be shown in Sec. III E, H^+ is more stable in *p*-type material than H_2, while H^- is always less stable. The same can be expected in hexagonal polytypes.

We also find that a H_{AB_C}-$H_{AB_{Si}}$ pair on two sides of the same Si-C bond is more stable than either a pair of isolated

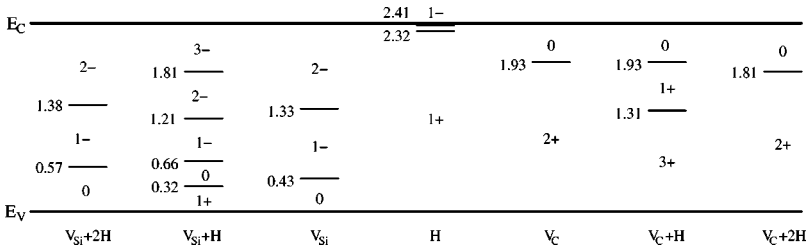

FIG. 5. The calculated occupation levels in 3*C*-SiC (+/0 occupation level probably exists in the gap for $V_{Si}+2H$ and V_{Si}, while a 2−/3− occupation level may also exist for the latter). The energies in eV of the occupation levels are given with respect to the valence band.

H^0 interstitials or isolated interstitial H^+ and H^-. The energy of this complex is higher than that of $(H_2)_{T_{Si}}$ only by 0.91 eV. The bond lengths are H-Si, 1.679 Å, Si-C, 2.139 Å, and C-H, 1.142 Å, showing that a strong C-H and a weaker Si-H bond are formed at the expense of almost dissociating the Si-C bond.

C. One or two hydrogen atoms in a silicon vacancy

The silicon vacancy (V_{Si}) is a deep acceptor in 3*C*-SiC. The negative charge state is characterized by T_d symmetry and $S=3/2$.[46] Our geometry for V_{Si}^0 (9.5% outward breathing[47]), as well as the formation energy (8.16 eV, see Table I) and the position of the highest occupied level (at $E_V+0.49$ eV, calculated without the gap correction in the 128-atom unit), agree fairly well with the corresponding values of Ref. 39 (9.1%, 8.45 eV, and $E_V+0.32$ eV). With all corrections applied, we obtain the highest occupied one-electron level at $E_V+0.76$ eV in the neutral and at $E_V+0.94$ eV in the negative charge state.[40]

The Jahn-Teller reconstruction is negligible in V_{Si} because of the localized nature of the carbon dangling bonds and the relatively long C-C distances across the vacancy. Due to the degeneracy of the highest occupied one-electron orbital ($\sim t_2$ in all charge states), a LDA-type calculation (with spin polarization) should necessarily result in high spin state configurations. However, it was shown that, in the ground state of V_{Si}^0, many-body effects lower the ^1E singlet ($S=0$) state below the ^3T triplet ($S=1$) one.[48] In a more recent self-consistent calculation, an energy difference of ~ 0.1 eV was found in favor of the singlet ground state.[49] Therefore, we corrected the energy of the triplet by -0.1 eV to get an estimate for the true ground state of V_{Si}^0. [The same will be done with $(V_{Si}+H)^-$.] With these corrections we estimate the (0/−/2−) occupation levels of V_{Si} in 3*C*-SiC to be around $E_V+0.43$ eV and $+1.33$ eV, respectively, from our 128-atom calculation.[50] Higher negative or positive charge states of V_{Si} may exist but have not been calculated. (All the calculated occupation levels are displayed together in Fig. 5.)

The bonding configuration of $(V_{Si}+H)^0$ is shown in Fig. 6. The hydrogen bonds to one of the carbon neighbors with a C-H distance of 1.12 Å. Unlike in diamond or silicon, however, the remaining carbon dangling bonds cannot form bonds to cause a significant Jahn-Teller distortion. (The relaxed distance between those carbon atoms is 3.38 Å, to be compared to a normal C-C bond length of 1.54 Å.) So the symmetry is close to C_{3v}, the C-H bond being only 0.3° off the [111] axis. The three dangling bonds give rise to an $a'(\approx a_1)$ orbital in the valence band and a nearly degenerate $a',a''(\sim e)$ pair in the lower half of the gap.[51] The latter is occupied only by one electron, which gives rise to acceptor activity. The position of this *e* level in $(V_{Si}+H)^-$—where it is doubly occupied—is at $E_V+0.83$ eV, i.e., closer to the CB than the t_2 of V_{Si}^-. It is interesting to note the analogies between the electronic structure of V_{Si}^+, which is close to T_d symmetry, and $(V_{Si}+H)^0$, which is close to C_{3v} symmetry. (Note that this symmetry difference disappears in hexagonal polytypes.) Both systems have one unpaired electron which occupies an otherwise empty degenerate level. The corresponding orbitals in the two systems are very similar. Spin density maps of the singly occupied orbitals are given in Fig. 7.

The (+/0/−/2−/3−) occupation levels of $(V_{Si}+H)$, estimated from the 128-atom calculation, are at $E_V+0.32$, $+0.66$, $+1.21$, and $+1.81$ eV, respectively (see Fig. 5). This implies that $(V_{Si}+H)$ is negatively charged in *n*-type 3*C*-SiC, i.e., it is a very effective electron trap. A similar behavior can be predicted for the hexagonal polytypes as well. Considering its (+/0) occupation level in 3*C*-SiC, interstitial H will be attracted by V_{Si} unless the sample is heavily *n* doped ($E_F>E_V+2.32$ eV, when H is neutral) or heavily *p* doped ($E_F<E_V+0.43$ eV, when V_{Si} is neutral). In hexagonal polytypes repulsion is likely for strong *n* doping. (Fermi level positions are understood at the temperature of annealing.) In a weakly *n*-type sample (say with E_F-E_V

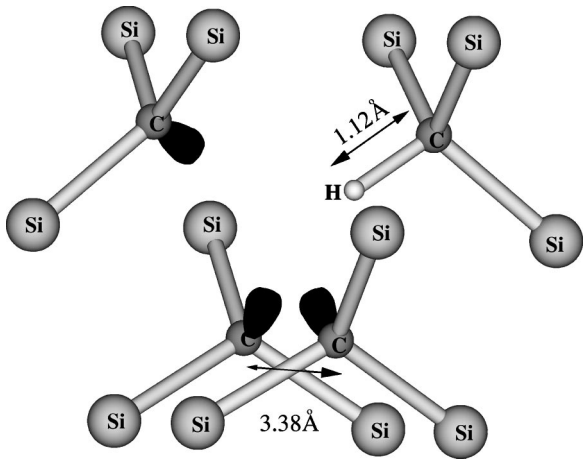

FIG. 6. The bonding configuration of a single hydrogen atom in a silicon vacancy of 3*C*-SiC.

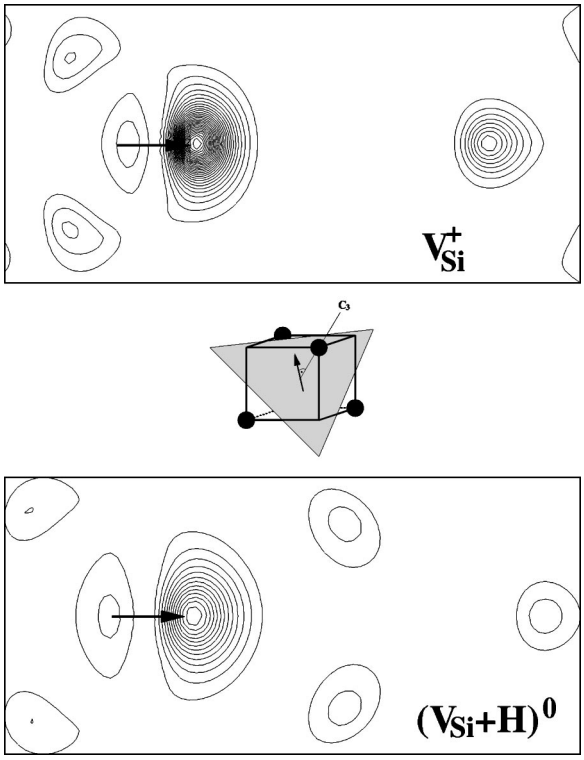

FIG. 7. The spin distribution in V_{Si}^{+} and $(V_{Si}+H)^{0}$ in the plane shown in the middle figure. The arrow serves to orient the figures. The contours connect points of equal density.

$=1.4$ eV) the energy gain upon the formation of a stable $(V_{Si}+H)^{2-}$ complex is (calculated from the total energies of the corresponding defects in the 128-atom unit)

$$V_{Si}^{2-}+H^{+} \xrightarrow{-[2.45+(E_F-E_V)]=-3.85\ \text{eV}} (V_{Si}+H)^{2-}+h^{+}. \quad (1)$$

This value can be regarded as a lower bound for the dissociation energy at this Fermi level position. A second hydrogen atom can also be trapped in V_{Si}, although the energy balance for neutral systems (p-type material) is approximately[52]

$$2\times(V_{Si}+H) \xrightarrow{+0.48\ \text{eV}} (V_{Si}+2H)+V_{Si}. \quad (2)$$

In the $(V_{Si}+2H)$ complex two carbon dangling bonds are saturated and the symmetry is C_{2v}. The other two dangling bonds give rise to a doubly occupied level very close to the valence band (VB) and an empty level in the lower half of the gap. Therefore, $(V_{Si}+2H)$ is still an acceptor and may exist as both $[V_{Si}+2H]^{-}$ and $[V_{Si}+2H]^{2-}$.[53] The $(0/-/2-)$ occupation levels are at $E_V+0.57$ and $+1.38$ eV, respectively. That means that we obtain both the $(0/-)$ and the $(-/2-)$ occupation levels of V_{Si}, $(V_{Si}+H)$, and $(V_{Si}+2H)$ within about 0.2 eV (see Fig. 5).

As a consequence further H^{+} interstitials can be attracted electrically to $(V_{Si}+2H)^{-q}$ in all but strongly p-type material. Only $(V_{Si}+4H)$ is expected to be electrically and chemically passive. $(V_{Si}+3H)$ and $(V_{Si}+4H)$ complexes are, however, increasingly metastable with respect to isolated $(V_{Si}+H)$ complexes (in p-type material):[52]

$$3\times(V_{Si}+H) \xrightarrow{+0.81\ \text{eV}} (V_{Si}+3H)+2\times V_{Si}, \quad (3)$$

$$4\times(V_{Si}+H) \xrightarrow{+1.34\ \text{eV}} (V_{Si}+4H)+3\times V_{Si}. \quad (4)$$

Therefore, they will be created only if $[H] \gg [V_{Si}]$. It is interesting to note, however, that

$$V_{Si}+H_2 \xrightarrow{-8.00\ \text{eV}} (V_{Si}+2H). \quad (5)$$

Therefore, molecules will be captured and dissociated by silicon vacancies.

The calculated stretching mode frequency of the C-H bond in $(V_{Si}+H)$ is 2961 cm^{-1}. Substituting H with D shifts the frequency to 2170 cm^{-1}. In $(V_{Si}+2H)$ the two C-H bonds gives rise to a symmetric and an asymmetric combination at 3051 and 2999 cm^{-1}, respectively. Substituting one H atom with D will shift them to 3014 and 2206 cm^{-1}, while $(V_{Si}+2D)$ will have frequencies at 2229 and 2200 cm^{-1}.

D. One or two hydrogen atoms in a carbon vacancy

The ''longer'' dangling bonds of Si in V_C easily make bonds between the vacancy neighbors (across an unrelaxed distance of a mere 3.1 Å), causing considerable Jahn-Teller distortion to D_{2d}. Our geometry (2.6% inward breathing and 7.7% pairing distortion[47]), as well as the formation energy (4.49 eV, see Table I) and the $(2+/0)$ occupation level (at $E_V+1.55$ eV, calculated without the gap correction in the 128-atom unit), agree very well with the corresponding results of Ref. 39 (2.8%, 10.6%, 4.30 eV, and $E_V+1.57$ eV). With all corrections applied, we obtain the $(2+/0)$ occupation level at $E_V+1.93$ eV. The $(0/-)$ occupation level is almost degenerate with the CB edge.[54]

Due to the Jahn-Teller distortions of V_C, which are similar to the vacancies in elemental semiconductors, a bonding configuration similar to that known from silicon[55,56] is expected in the case of (V_C+H), i.e., hydrogen saturating one of the Si dangling bonds, two other dangling bonds forming a long bond (causing significant pairing of the Si atoms concerned), and one dangling bond remaining (C_{1h} symmetry). However, for the (V_C+H) complex in SiC (both $3C$ and $4H$), the situation is very different.[29] The C_{1h} structure with one Si-H bond turns out to be metastable. Hydrogen in a symmetric position (C_{2v}) between two Si atoms, forming a three-center bond (see Fig. 8), is more stable by 0.5 eV in the 32-atom calculation. The resulting electronic structure is very similar to that of the bond-center H interstitial in silicon and diamond. The electron density shows that the two-center long bond between two Si neighbors of the reconstructed carbon vacancy becomes a three-center bond, enveloping the H atom between the two Si atoms. The one-electron level corresponding roughly to this bond is in the valence band. The electron introduced by the H atom finds its place on the

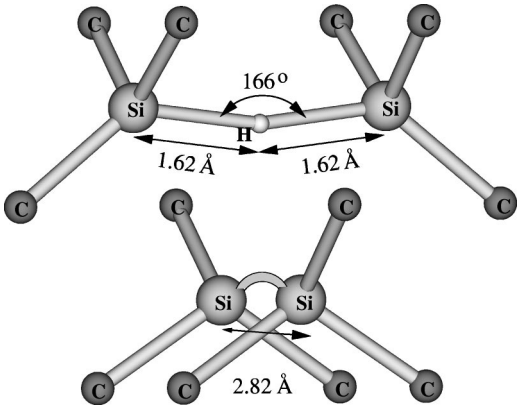

FIG. 8. The bonding configuration of a single hydrogen atom in a carbon vacancy in 3*C*-SiC.

antibonding combination of the sp^3 hybrids of its neighbors, so that the H atom is at the node of this orbital. The overcoordinated bond-center interstitial is unique to elemental semiconductors.[22] SiC seems to be the first example for H entering a three-center bond when trapped in a vacancy. The reason probably is that the Si-Si distance across the carbon vacancy in SiC is about 3.1 Å, while the normal Si-H bond length is ~1.5 Å, so the H atom can interact with at least two Si atoms. Still, this alone does not explain the preference of H for the three-center bonded configuration over the normal two-center bonded one (where the Si-H bond distance is 1.46 Å and H is about 2.2 Å away from the silicon atom with the dangling bond). It is interesting to note that the relaxed Si-Si distance around H_{BC} in Si is 3.2 Å,[27] i.e., almost identical with the Si-Si distance, 3.1 Å, across the unrelaxed carbon vacancy in SiC. The three-center bonded configuration of Fig. 6 can be formed without significant relaxation of the host atoms, while the two-center bonded configuration is accompanied by a 7% outward relaxation of the Si atom with the dangling bond. This also means, however, that the energy of a three-center bonded Si-H-Si unit is comparable—within the order of the relaxation energies (a few tenths of an eV)—to the energy of the two-center bonded Si-H unit and a Si dangling bond.

The one singly and the one doubly occupied level associated with neutral (V_C+H) in the gap of 3*C*-SiC (the latter corresponds to the long bond in Fig. 8) allow in principle the existence of three positive charge states, (1+), (2+), and (3+). $(V_C+H)^+$ has essentially the same structure as the neutral defect (0.3 eV more stable than the configuration with the two-center Si-H bond). In the double positive state, the two configurations are nearly equally stable (within 0.05 eV), while in the (3+) state a very weak single Si-H bond and three empty dangling bonds establish C_{3v} symmetry. In other words the (V_C+H) system is bistable. We have calculated the relative stabilities of the different charge states as a function of the Fermi level position (see Figs. 5 and 9). The (2+) charge state is not stable for any Fermi level position, i.e., the system shows negative *U* behavior. The calculated (3+/1+/0) occupation levels are at $E_V+1.31$ and $+1.93$ eV. The latter is within 0.01 eV of the value obtained for the (2+/0) level of V_C. It should also be noted that the $(V_C+H)^0$ complex has similar electronic structure to V_C^-. Spin density maps of the singly occupied orbitals are given in Fig. 10. As can be seen the spin distribution is nearly identical for the two complexes.

Considering the occupation levels of interstitial H and V_C, it can be seen that they do not repel each other only for $E_V+1.93<E_F<2.40$ eV, but at no position of the Fermi level is there attraction between them. [The latter will be more or less true for hexagonal polytypes, since we expect the (0/−) or (0/2−) occupation level of V_C to appear in the larger gaps around $E_V+2.4$ eV, where the +/− occupation level of H is expected as well.] In *p*-type material formation of the complex from isolated V_C and H_i is retarded due to the Coulomb repulsion. However, if it is created, e.g., in epitaxial growth, the $(V_C+H)^{3+}$ complex is stable with respect to the isolated constituents. From the total energies of the corresponding defects obtained in the 128-atom unit,

$$(V_C+H)^{3+} \overset{+1.26\ \text{eV}}{\rightarrow} V_C^{2+}+H^+, \tag{6}$$

which is about 1/3 of the binding energy of H to V_{Si}. The weak bonding is characteristic of the (3+) charge state. In *n*-type material, say at $E_F-E_V=2.0$ eV, the bonding energy of H in V_C (the lower bound to dissociation) is

$$(V_C+H)^0 \overset{+[0.56+(E_F-E_V)]=+2.56\ \text{eV}}{\longrightarrow} V_C^0+H^++e^-, \tag{7}$$

which is, however still less than 2/3 of the value obtained in Eq. (1). So, if both types of vacancy are present in sufficient concentration, interstitial hydrogen prefers complex formation with V_{Si} over V_C both kinetically and thermodynamically under equilibrium conditions.

Introducing a second hydrogen into V_C establishes another three-center bonded configuration between the other

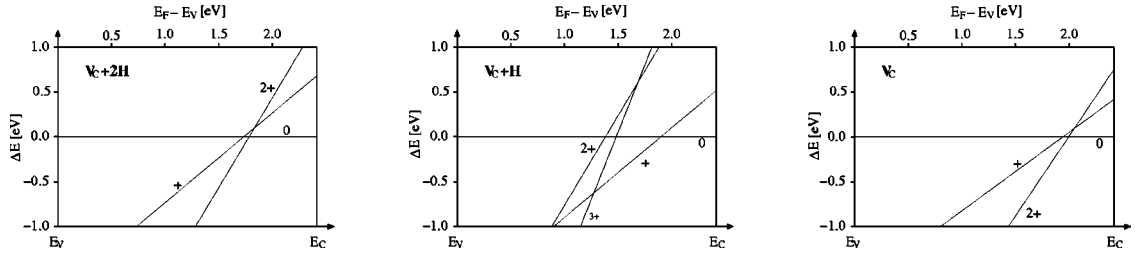

FIG. 9. The stability of the charged states of (V_C+nH) defects with respect to the neutral state. At any position of the Fermi level the charge state with the lowest energy is stable. All three systems show negative *U* behavior, but only V_C+H is bistable.

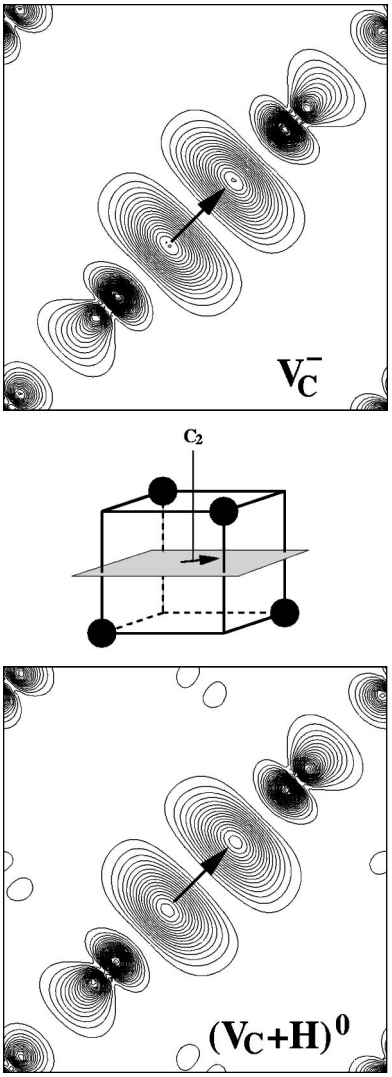

FIG. 10. The spin distribution in V_C^- and $(V_C+H)^0$ in the plane shown in the middle figure. The arrow serves to orient the figures. The contours connect points of equal density.

two Si neighbors of the vacancy (see Fig. 11). The Si-H-Si bridges become more puckered: the angle being 155° with Si-H distances of 1.64 Å and a H-H distance of 1.61 Å. The system is most probably a biradical (two electrons with opposite spins on two spatially orthogonal antibonding orbitals) with D_{2d} symmetry. A biradical is beyond the scope of a one-electron theory, like the LDA, so we have calculated the triplet state of the defect in D_{2d} symmetry instead (two electrons with parallel spin on two spatially orthogonal antibonding orbitals). The system is a double donor with a doubly degenerate e state 0.23 eV below the CB edge.

We have also calculated the singly and doubly positive charge states of (V_C+2H). If $(V_C+2H)^0$ is calculated in the singlet state, the geometry distorts from D_{2d} to D_2 (and the energy is higher than that of the triplet state). $(V_C+2H)^+$ preserves the D_2 symmetry (with a small margin over C_{2v}), while $(V_C+2H)^{2+}$ is D_{2d} again. In order to calculate the occupation levels, we have assumed that $(V_C+2H)^0$ has a D_{2d} singlet many-electron ground state (just as V_{Si}^0 has a T_d

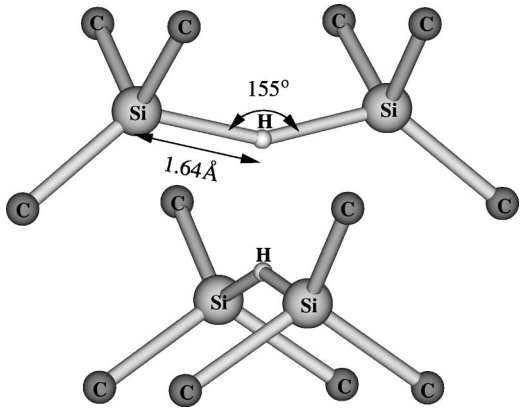

FIG. 11. The bonding configuration of two hydrogen atoms in a carbon vacancy of 3C-SiC.

singlet one), and this is also $\sim$0.1 eV more stable than the triplet in the same symmetry (as was obtained for V_{Si}^0 in Ref. 49). Comparison of the energies as a function of the Fermi level position shows that the system has a negative U behavior, i.e., $(V_C+2H)^+$ is never stable in equilibrium. The (2+/0) occupation level is around $E_V+1.81$ eV, with an uncertainty in this case somewhat larger than ± 0.15 eV. It is interesting to note that all V_C-based systems investigated show negative U behavior (Fig. 9). For V_C and (V_C+2H) this originates from the reconstruction caused by the long-bond formation between dangling bonds, and is similar to the case of vacancies in elemental semiconductors. In the case of (V_C+H) the reason is a change in the bonding of hydrogen, and the instability of the paramagnetic $(V_C+H)^{2+}$ state is much more pronounced. The paramagnetic V_C^+ and $(V_C+2H)^+$ are only marginally unstable, and are likely to be detectable by EPR under nonequilibrium conditions (e.g., under illumination). These centers have similar spin distributions, as can be seen on the spin density maps of the singly occupied orbitals in Fig. 12.

Since both (V_C+nH) complexes are donors and the capture of a third hydrogen atom is energetically not feasible, V_C cannot be passivated by hydrogen. This is again unusual among semiconductors. The (V_C+nH) centers are always positively charged in p-type material, i.e., they are effective hole traps. (This will apply for hexagonal polytypes, too.)

The formation energy per H atom is lower in (V_C+2H) than in (V_C+H) at any position of the Fermi energy. The emission of H from (V_C+2H) can be described by the reaction

$$(V_C+2H)^{2+}+2\times h^+ \xrightarrow{+[0.03+2(E_F-E_V)]} (V_C+H)^{3+}+H^+ \tag{8}$$

in p-type and by

$$(V_C+2H)^{2+/0} \xrightarrow{+4.0} (V_C)^{2+/0}+H_2 \tag{9}$$

in n-type 3C material. These equations show that once the (V_C+2H) complex is formed, it remains stable against inter-

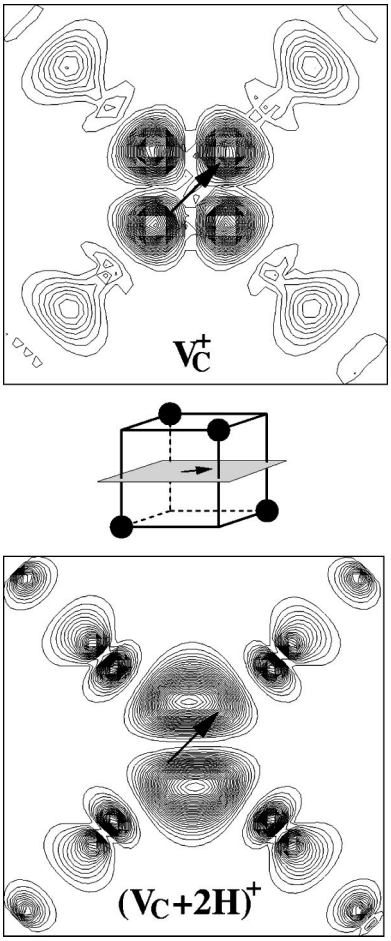

FIG. 12. The spin distribution in V_C^+ and $(V_C+2H)^+$ in the plane shown in the middle figure. The arrow serves to orient the figures. The contours connect points of equal density.

stitial hydrogen emission. However, if an excess of carbon vacancies is available, then in *p*-type material

$$(V_C+2H)^{2+}+V_C^{2+}+2\times h^+ \xrightarrow{+[-1.23+2(E_F-E_V)]} 2\times(V_C+H)^{3+}, \quad (10)$$

i.e., single-hydrogen complexes are more favorable energetically in *p*-type 3*C*-SiC. The reverse of Eq. (9) also shows that V_C can dissociate H_2 molecules as well, although less effectively than V_{Si}.

In the neutral charge state of (V_C+H), the Si-H-Si unit has an asymmetric and a symmetric stretch mode at 1570 and 991 cm^{-1}, respectively. Both are IR and Raman active. In the singly positive charge state, the loss of an electron from an antibonding orbital stiffens the stretch modes to 1770 and 1189 cm^{-1}. In the doubly positive charge state, the two-center Si-H bond is characterized by a ''normal'' Si-H stretch mode of 2072 cm^{-1}. For the triply positive state the geometry obtained with the Gaussian basis differed too much from the one obtained with the plane wave basis, so the calculated frequency could be questionable. The puckering of the Si-H-Si units in neutral (V_C+2H) softens the degenerate asymmetric stretch modes to 976 cm^{-1}, and gives rise to a strong splitting between the symmetric and antisymmetric combination of the two symmetric ones. The Raman active symmetric combination is at 1332 cm^{-1}. In the doubly positive state these frequencies shift to 1132 and 1205 cm^{-1}, respectively. It has to be noted that some of these LVM's are very close to the continuum of SiC vibrations, so the accuracy is probably less than usual.

E. Formation energies of the one- and two-hydrogen defects in 3*C*-SiC

The main motivation of our comparative study of hydrogen defects is to establish their relative stability. For this purpose, a formation energy can be defined based on the total energies calculated for the equilibrium of a system consisting of n_{Si} silicon, n_C carbon, and n_H hydrogen atoms in the q charge state (see, e.g., Refs. 39 and 57):

$$E^q_{form}(n_{Si},n_C,n_H;\mu_{Si},\mu_C,\mu_H,E_F) = E^q_{tot}(n_{Si},n_C,n_H)-n_{Si}\mu_{Si}-n_C\mu_C-n_H\mu_H+qE_F. \quad (11)$$

Here E_F is the Fermi energy (in other words the chemical potential of the electrons), i.e., the energy of the reservoir from which electrons are taken, which depends on the doping level and temperature of the real crystal. Similarly, μ_H is the chemical potential of H, i.e., the energy of the reservoir from which H atoms are taken: H_2 or atomic hydrogen gas in equilibrium with the SiC crystal. It has to be taken into account that, in equilibrium with the SiC crystal, the chemical potentials of silicon, μ_{Si}, and carbon, μ_C, are connected by the relation

$$\mu_{Si}+\mu_C=\mu^{bulk}_{SiC}. \quad (12)$$

Introducing

$$\Delta\mu_{Si}=\mu_{Si}-\mu^{bulk}_{Si}, \quad \Delta\mu_C=\mu_C-\mu^{bulk}_C, \quad (13)$$

and taking into account that the formation enthalpy of SiC is

$$\Delta H^{SiC}_f=\mu^{bulk}_{SiC}-(\mu^{bulk}_{Si}+\mu^{bulk}_C), \quad (14)$$

it follows that

$$\Delta\mu_{Si}+\Delta\mu_C=\Delta H^{SiC}_f. \quad (15)$$

Defining[58]

$$\Delta\mu=\Delta\mu_{Si}-\frac{1}{2}\Delta H^{SiC}_f=\frac{1}{2}\Delta H^{SiC}_f-\Delta\mu_C, \quad (16)$$

Eq. (11) can be rewritten as

$$E^q_{form}(n_{Si},n_C,n_H;\mu_{Si},\mu_C,\mu_H,E_F) = \Delta E^q(n_{Si},n_C,n_H)-(n_{Si}-n_C)\Delta\mu-n_H\mu_H+qE_F, \quad (17)$$

where the environment-independent relative energy of the defect

$$\Delta E^q(n_{\mathrm{Si}},n_{\mathrm{C}},n_{\mathrm{H}})=\left[E^q_{\mathrm{tot}}(n_{\mathrm{Si}},n_{\mathrm{C}},n_{\mathrm{H}})-\frac{(n_{\mathrm{Si}}+n_{\mathrm{C}})}{2}\mu^{\mathrm{bulk}}_{\mathrm{SiC}}-\frac{(n_{\mathrm{Si}}-n_{\mathrm{C}})}{2}(\mu^{\mathrm{bulk}}_{\mathrm{Si}}-\mu^{\mathrm{bulk}}_{\mathrm{C}})\right] \tag{18}$$

does not contain either the chemical potential of the constituent atoms or that of the electrons. The chemical potentials in the bulk were calculated as the energy per formula unit of the perfect SiC, silicon, and diamond supercells. (The small difference in the energy of graphite and diamond does not introduce significant error.) Using these values, Eq. (14) gives $\Delta H_{\mathrm{f}}^{\mathrm{SiC}}=-0.64(-0.71)$ eV in the 32- (128-)atom cells, to be compared to the experimental value of -0.72 eV.[59]

The tuning of the C/Si ratio during growth is theoretically limited by ($\mu_{\mathrm{C}}=\mu_{\mathrm{C}}^{\mathrm{bulk}}$) for C-rich conditions, and by ($\mu_{\mathrm{Si}}=\mu_{\mathrm{Si}}^{\mathrm{bulk}}$) for Si-rich conditions. So from Eqs. (13), (15), and (16) it follows that

$$+\frac{1}{2}\Delta H_{\mathrm{f}}^{\mathrm{SiC}}\leqslant\Delta\mu\leqslant-\frac{1}{2}\Delta H_{\mathrm{f}}^{\mathrm{SiC}}. \tag{19}$$

The total energy $E^q_{\mathrm{tot}}(n_{\mathrm{Si}},n_{\mathrm{C}},n_{\mathrm{H}})$ in Eq. (18) is calculated as

$$E^q_{\mathrm{tot}}(n_{\mathrm{Si}},n_{\mathrm{C}},n_{\mathrm{H}})=E^q_{\mathrm{SCM}}(n_{\mathrm{Si}},n_{\mathrm{C}},n_{\mathrm{H}})+E^q_{\mathrm{ZP}}(\mathrm{H}) \tag{20}$$

where $E^q_{\mathrm{SCM}}(n_{\mathrm{Si}},n_{\mathrm{C}},n_{\mathrm{H}})$ is the total energy of the supercell containing the defect with charge q, and $E^q_{\mathrm{ZP}}(H)$ is the energy due to the zero point vibrations of the hydrogen atoms in that charge state.[60] Table II shows calculated formation energies defined in Eq. (17) for the limiting cases in Eq. (19), as a function of the hydrogen chemical potential within the stability limits set by the occupation levels in equilibrium (as shown in Fig. 5). (Positive values mean that the formation is endothermic.) The $E^q_{\mathrm{SCM}}(n_{\mathrm{Si}},n_{\mathrm{C}},n_{\mathrm{H}})$ values calculated in the 128-atom SCM were corrected for the spin-polarization error, as explained at the end of Sec. II. In the cases of V^0_{Si}, $(V_{\mathrm{Si}}+\mathrm{H})^-$, and $(V_{\mathrm{C}}+2\mathrm{H})^0$, an additional 0.1 eV was subtracted to estimate the energy of the singlet state from the LDA result on the triplet (cf. Sec. III C).

In order to evaluate Table II, an expression for μ_{H} is needed. The chemical potential of hydrogen gas (both molecular and atomic) strongly depends on temperature and pressure. For μ_{H} with respect to H_2 and H gases we use the formulas of Ref. 61, leading to

$$2\,\mu_{\mathrm{H}}(\mathrm{H}_2)=E(\mathrm{H}_2)+8.617\,386\times10^{-5}T\ln[1.267\,865\times10^3 p\,T^{-7/2}(1-e^{-(6.301215\times10^3)/T})]+0.2715, \tag{21}$$

$$\mu_{\mathrm{H}}(\mathrm{H})=E(\mathrm{H})+8.617\,386\times10^{-5}T\ln(19.314\,058\,p\,T^{-5/2}). \tag{22}$$

Here $E(\mathrm{H}_2)=-30.58$ eV and $E(\mathrm{H})=-13.03$ eV are the energies of the H_2 molecule and of the H atom, respectively, calculated (with spin polarization in the latter case) in a large supercell geometry using the same cutoff as in the crystal.[62] p and T denote pressure and temperature given in atm and K, respectively. Reasonable values of μ_{H} range between -13 and -17 eV.

Another parameter in Eq. (17) and in Table II is the actual position of the Fermi level, which depends not only on the temperature and dopant concentration, but also on the concentration of the defects under study. Therefore, it has to be determined self-consistently from the neutrality condition

$$n+\sum_i|q_i|(N_{\mathrm{A}i}-p_{\mathrm{A}i})=p+\sum_i|q_i|(N_{\mathrm{D}i}-n_{\mathrm{D}i}) \tag{23}$$

where[63]

$$n=N_{\mathrm{C}}e^{-(E_{\mathrm{C}}-E_{\mathrm{F}})/k_{\mathrm{B}}T},\quad p=N_{\mathrm{V}}e^{-(E_{\mathrm{F}}-E_{\mathrm{V}})/k_{\mathrm{B}}T} \tag{24}$$

are the electron and hole concentrations in the CB and VB, respectively. The effective density of states has been calculated with the longitudinal and transversal electron masses[64] $0.247\,m_0$ and $0.677\,m_0$ for the CB (N_{C}) and with the heavy and light hole masses[65] $1.109m_0$ and $0.331m_0$ for the VB (N_{V}). The terms in parentheses in the summation on both sides of Eq. (23) are the concentrations of ionized acceptors and donors (including all the electrically active H-related defects). $N_{\mathrm{A}i}$ and $N_{\mathrm{D}i}$ are the total concentrations of acceptors and donors, respectively, while $p_{\mathrm{A}i}$ ($n_{\mathrm{D}i}$) is the concentration of holes (electrons) in the acceptor (donor) states. The concentration of dopants and the temperature (T) were used as free parameters, and the concentration of defects was estimated by

$$N_i=N_i^0e^{-E^{q_i}_{\mathrm{form}}/k_{\mathrm{B}}T}, \tag{25}$$

i.e., assuming noninteracting defects and neglecting the entropy term in the heat of formation (N_i^0 is the concentration of sites in the perfect lattice for the given defect). Once Eq. (23) is solved, Eq. (25) supplies the equilibrium defect concentrations.

IV. DISCUSSION

A. Hydrogenation of SiC

Of course, the most interesting question is which (if any) of the defects described in the previous sections will be formed under given experimental conditions, i.e., when and how much hydrogen can be expected in the crystal? We are not aware of any direct study on the hydrogenation of $3C$-SiC, but—as listed in the Introduction—there is a number of reports, based on direct (SIMS) or indirect (dopant passivation) evidence, regarding the hydrogen content of $4H$- and $6H$-SiC samples. In principle, our results allow us to discuss only the situation in $3C$-SiC, and even there only rough estimates can be given for the hydrogen concentrations. The uncertainties in our calculations may lead to almost order of magnitude differences in the concentrations. Still, the general dependence of H incorporation on temperature and doping can be predicted and even qualitative extrapolation to hexagonal polytypes is possible. The extrapolation is based on the following argument.

TABLE II. Defect formation energies in 3*C*-SiC, as defined by Eqs. (17)–(20). The general error bar in relative stabilities and in the position of the occupation level is expected to be ± 0.15 eV, except for the lines marked with a,b, where additional sources of uncertainity exist. Reasonable values of μ_H range between -13 and -17 eV. Ellipses indicate, that higher charge states may exist, but have not been calculated.

Defect	Stability range ($E_F - E_V$) (eV)	E^q_{form} (eV) $\mu_{Si}=\mu_{Si}^{bulk}$ (Si rich)	$\mu_C=\mu_C^{bulk}$ (C rich)
V_C^{2+}	0.00 – 1.93	1.05 – 4.90	1.76 –5.61
V_C^{0}	1.93 – 2.41	4.90 – 4.90	5.61 – 5.61
$(V_C+H)^{3+}$	0.00 – 1.31	$(-14.45-\mu_H)$ –$(-10.52-\mu_H)$	$(-13.75-\mu_H)$ –$(-9.81-\mu_H)$
$(V_C+H)^{1+}$	1.31 – 1.93	$(-10.52-\mu_H)$ –$(-9.90-\mu_H)$	$(-9.81-\mu_H)$ – $(-9.20-\mu_H)$
$(V_C+H)^{0}$ [a]	1.93 – 2.41	$(-9.90-\mu_H)$ – $(-9.90-\mu_H)$	$(-9.20-\mu_H)$ – $(-9.20-\mu_H)$
$(V_C+2H)^{2+}$	0.00 – 1.81	$2\times(-14.36-\mu_H)$ – $2\times(-12.55-\mu_H)$	$2\times(-14.01-\mu_H)$ – $2\times(-12.20-\mu_H)$
$(V_C+2H)^{0}$ [a, b]	1.81 – 2.41	$2\times(-12.55-\mu_H)$ – $2\times(-12.55-\mu_H)$	$2\times(-12.20-\mu_H)$ –$2\times(-12.20-\mu_H)$
V_{Si}^{0} [a, b]	··· –0.43	8.87 – 8.87	8.16 – 8.16
V_{Si}^{1-} [a]	0.43 – 1.33	8.87 –7.97	8.16 – 7.26
V_{Si}^{2-} [a]	1.33 – ···	7.97 –···	7.26 – ···
$(V_{Si}+H)^{0}$ [a]	0.32 – 0.66	$(-7.94-\mu_H)$ – $(-7.94-\mu_H)$	$(-8.64-\mu_H)$ – $(-8.64-\mu_H)$
$(V_{Si}+H)^{1-}$ [a, b]	0.66 – 1.21	$(-7.94-\mu_H)$ – $(-8.49-\mu_H)$	$(-8.64-\mu_H)$ – $(-9.19-\mu_H)$
$(V_{Si}+H)^{2-}$ [a]	1.21 – 1.81	$(-8.49-\mu_H)$ – $(-9.69-\mu_H)$	$(-9.19-\mu_H)$ – $(-10.39-\mu_H)$
$(V_{Si}+H)^{3-}$	1.81 – 2.41	$(-9.69-\mu_H)$ – $(-11.49-\mu_H)$	$(-10.39-\mu_H)$ – $(-12.19-\mu_H)$
$(V_{Si}+2H)^{0}$	··· – 0.57	$2\times(-12.48-\mu_H)$ – $2\times(-12.48-\mu_H)$	$2\times(-12.83-\mu_H)$ – $2\times(-12.83-\mu_H)$
$(V_{Si}+2H)^{1-}$ [a]	0.57 – 1.38	$2\times(-12.48-\mu_H)$ – $2\times(-12.89-\mu_H)$	$2\times(-12.83-\mu_H)$ – $2\times(-13.24-\mu_H)$
$(V_{Si}+2H)^{2-}$	1.38 – 2.41	$2\times(-12.89-\mu_H)$ – $2\times(-13.92-\mu_H)$	$2\times(-13.24-\mu_H)$ – $2\times(-14.27-\mu_H)$
$(H_2)_{T_{Si}}$	0.00 – 2.41	$2\times(-12.91-\mu_H)$	
$H^{+}_{AB_C}$	0.000 – 2.320	$(-14.255-\mu_H)$ — $(-11.935-\mu_H)$	
$H^{0}_{AB_C}$	2.320 – 2.405	$(-11.935-\mu_H)$ — $(-11.935-\mu_H)$	
$H^{-}_{T_{Si}}$	2.405 – 2.410	$(-11.935-\mu_H)$ — $(-11.940-\mu_H)$	

[a]The values used here were corrected for the spin-polarization error, as explained at the end of Sec. II.

[b]An additional 0.1 eV was subtracted to estimate the energy of the many-electron singlet state from the LDA result on the triplet, as explained in Sec. III C.

(i) The stability of a charged complex may vary within several eV, depending on the position of the Fermi level. As can be seen from Table II, neutral hydrogen complexes typically have a rather high formation energy. The formation energy decreases in the positively charged states because energy is gained by having promoted electrons from the defect to the Fermi level if the latter lies lower. Similarly, in the negatively charged states, energy is gained by having promoted electrons from the Fermi level to the defect if the former lies higher. The highest concentration of the defects, therefore, occurs for the highest charge state at the highest level of doping, i.e., when E_F is farthest from the occupation level (theoretically at $E_F=E_V$ or $E_F=E_C$). Since the VB offset is very small between the polytypes, assuming a nearly identical position for the $+/0/-$ occupation levels of a given defect with respect to the VB edges (and no higher charge states), the formation energy of the positive defect will be about the same in all polytypes, while the negative defect can decrease its energy in the hexagonal polytypes because E_F can move farther up.

(ii) We know from Refs. 38 and 39 that the formation energy of the neutral vacancies changes by less than 0.4 eV, while the (uncorrected) occupation levels differ only by less than 0.1 eV between the 3*C*- and 4*H*-polytypes. Based on the convergence properties shown in Table I, the $(V+nH)$ defects appear to be more localized than pure vacancies. Therefore, we expect that the polytype dependence of the occupation levels and formation energies for these defects will not be bigger than our error bar in the 128-atom 3*C*-SiC calculation. In the case of interstitial H, we predicted a $(+/-)$ occupation level at around $E_V+2.4$ eV but little change in the energy of the charged states (Sec. III A). We expect no significant difference between the polytypes for H_2. Therefore, the conclusions drawn about defects in *p*-type 3*C*-SiC are qualitatively valid also in *p*-type 6*H*- and 4*H*-SiC. In *n*-type material, significantly higher stability and 1–2 orders of magnitude higher concentration of negatively charged complexes can be expected in hexagonal polytypes than in 3*C*-SiC.

Hydrogen can be introduced into SiC during epitaxial CVD growth, by hydrogen-plasma treatment, by annealing in H_2 gas, or by H^+ (D^+,H_2^+,D_2^+) implantation. These possibilities will be investigated in the following.

1. CVD epilayers

CVD growth proceeds at atmospheric pressure at around $1400-1500\,^{\circ}C$ and the source gases (mostly silane and propane) are usually introduced by diluting a few percent of them in a H_2 carrier gas (see, e.g., Ref. 6). Although, strictly

TABLE III. Calculated concentrations of hydrogen defects ($>10^{12}$ cm^{-3}) in 3*C*-SiC assuming equilibrium with hydrogen gas under CVD growth conditions. [H_i] is the interstitial hydrogen concentration, [$V+n$H] and [V] mean the concentrations of all the charged (V_C+nH) and V_C defects in *p*-type and all the charged ($V_{Si}+n$H) and V_{Si} defects in *n*-type material (all others are negligible under the given conditions). E_F-E_V is the Fermi level position with respect to the VB edge under the given conditions.

Conditions	Net carrier conc. (cm^{-3})	*p*-type (B_{Si}), $\mu_C=\mu_C^{bulk}$ 10^{19}	10^{18}	10^{17}	10^{16}	*n*-type (N_C), $\mu_{Si}=\mu_{Si}^{bulk}$ 10^{16}	10^{17}	10^{18}	10^{19}
1400 °C	E_F-E_V (eV)	0.57	0.90	1.18	1.26	1.28	1.36	1.65	1.96
1 atm H_2	[H_i]	5.7×10^{14}	6.1×10^{13}	8.5×10^{12}	4.8×10^{12}	4.3×10^{12}	2.4×10^{12}		
$\mu_H=-16.51$ eV	[$V+n$H]								
	[V]	8.8×10^{13}	1.0×10^{12}						
1400 °C	E_F-E_V (eV)	0.57	0.90	1.18	1.26	1.28	1.36	1.65	1.96
0.01 atm (H)	[H_i]	3.0×10^{16}	3.2×10^{15}	4.5×10^{14}	2.5×10^{14}	2.2×10^{14}	1.3×10^{14}	1.8×10^{13}	2.0×10^{12}
$\mu_H=-15.94$ eV	[$V+n$H]								
	[V]	8.8×10^{13}	1.0×10^{12}						
1500 °C	E_F-E_V (eV)	0.62	0.96	1.22	1.27	1.28	1.33	1.59	1.92
0.01 atm H	[H_i]	1.5×10^{16}	1.6×10^{15}	3.0×10^{14}	2.1×10^{14}	2.0×10^{14}	1.4×10^{14}	2.6×10^{13}	3.0×10^{12}
$\mu_H=-16.14$ eV	[$V+n$H]								
	[V]	1.5×10^{14}	1.7×10^{12}						

speaking there is no equilibrium during growth, a stationary state can be assumed between the concentrations of hydrogen in the gas phase and hydrogen in the crystal. At the temperature of CVD growth a fraction of the H_2 carrier gas dissociates. In the vicinity of the surface the incorporation reactions of the host and dopant atoms (from the precursor molecules) also release atomic hydrogen. We may assume about 1% atomic H in the vicinity of the surface. Table III shows the estimated hydrogen concentrations in as-grown 3*C*-SiC, assuming equilibrium with either 1 atm of H_2 at 1400 °C, or with 0.01 atm of H at 1400 and 1500 °C, for net carrier concentrations between 10^{16} and 10^{19} cm^{-3} in B-doped *p*-type and N-doped *n*-type material. All calculated concentrations above 1×10^{12} cm^{-3} are given in Table III. It is apparent that detectable concentrations of hydrogen complexes occur only in *p*-type material and the atomic hydrogen content of the gas is responsible for most of the incorporation. In *p*-type material ($N_A-N_D>0$), the most abundant hydrogen defect created during growth is the atomic (positively charged) interstitial. The hydrogen concentration increases monotonically with the net hole concentration.

In *p*-type 6*H*-SiC samples it was shown by SIMS that hydrogen incorporation follows the boron concentration closely[6] with [H] having the same order of magnitude as [B]. It was assumed that boron and hydrogen are grown into the sample as a complex. For samples with [B]$=1\times10^{18}$ cm^{-3} the net carrier concentration was found to be [p]$=3.5\times10^{17}$ cm^{-3}. Under such conditions our calculations predict an interstitial hydrogen concentration of 1×10^{16} cm^{-3}. If we assume that hydrogen grows into the lattice next to a boron atom [which was not considered in Eq. (23) but is quite reasonable because of the B_2H_6 source] its energy of incorporation is lowered by the binding energy of the complex. Assuming a $(+/-)$ occupation level for H_i at $E_V+2.4$ (Sec. III A) in 6*H*-SiC, our Eqs. (23)–(25) require a decrease of about 0.8 eV in the formation energy, to obtain a hydrogen concentration of 10^{18} cm^{-3}. This gives an estimate of the binding energy of such a (B+H) complex. Even if we do not assume the formation of a chemically bonded complex, a positive charge placed at the T_{Si} site next to B^- on the Si site in the unrelaxed lattice would give rise to a Coulomb attraction of 0.8 eV. In that sense, our result is consistent with the measurement and assumption of close (B+H) pairs of Ref. 6. In *n*-type 3*C*-SiC our results imply that the hydrogen incorporation appears to be negligible during growth. [This seems to hold for hexagonal polytypes as well, even with the higher stability of negatively charged defects. Assuming no change in the position of occupation levels but simply increasing the gap in Eq. (23) to 3.25 eV (4*H*-SiC) gives ($V_{Si}+n$H) concentrations on the order of 10^{11-12} cm^{-3}.] It is interesting to note the trends in the formation energy of the neutral vacancy-type defects upon hydrogenation. As can be calculated from Table II, in the case of (V_C+nH), the formation energy at 1400 °C in equilibrium with 0.01 atm atomic H ($\mu_H=-15.94$ eV) under Si-rich conditions increases from 4.90 to 6.04 to 7.78 eV, while in the case of ($V_{Si}+n$H) the formation energy under C-rich but otherwise the same conditions decreases from 8.16 eV to 7.30 to 6.22 eV for $n=0,1,2$ respectively. The reason is that some of the energy needed to create the vacancy and introduce a H atom into the crystal is regained by the formation of C-H or Si-H bonds in the hydrogenated vacancy. In the case of ($V_{Si}+n$H), the strong C-H bonds offset the energy of interstitial H incorporation, while in (V_C+nH) the weaker Si-H bonds do not. In a hydrogen-free environment the formation energy of V_{Si}^0 is 2.55 eV higher than that of V_C^0 even under C-rich conditions, whereas in the presence of hydrogen the formation energy of $(V_{Si}+2H)^0$ becomes 0.63 eV lower than that of $(V_C+2H)^0$. Since n can go up to 4 in ($V_{Si}+n$H) but only to 2 in (V_C+nH), the presence of hydrogen is expected not only to reverse the relative concentrations of V_C- and V_{Si}-type defects but to cause the concentration of (hydrogenated) silicon vacancies to increase to

TABLE IV. Calculated concentrations of hydrogen defects ($>10^{12}$ cm^{-3}) in 3*C*-SiC assuming equilibrium of the stoichiometric crystal with hydrogen gas. $[V+n\mathrm{H}]$ and $[V]$ mean the concentrations of all the charged ($V_\mathrm{C}+n\mathrm{H}$) and V_C defects in *p*-type and all the charged ($V_\mathrm{Si}+n\mathrm{H}$) and V_Si defects in *n*-type material (all others are negligible under the given conditions). $E_\mathrm{F}-E_\mathrm{V}$ is the Fermi level position with respect to the VB edge under the given conditions.

Conditions	Net carrier conc. (cm^{-3})	*p*-type (B_Si), $\mu_\mathrm{C}=\mu_\mathrm{Si}$				*n*-type (N_C), $\mu_\mathrm{C}=\mu_\mathrm{Si}$			
		10^{19}	10^{18}	10^{17}	10^{16}	10^{16}	10^{17}	10^{18}	10^{19}
300 °C	$E_\mathrm{F}-E_\mathrm{V}$ (eV)	0.90	1.02	1.13	1.24	1.71	1.77	1.83	1.89
0.03 atm H	$[\mathrm{H}_i]$	1.0×10^{19}	9.8×10^{17}	1.0×10^{17}	1.0×10^{16}				
$\mu_\mathrm{H}=-13.84$ eV	$[V+n\mathrm{H}]$	2.5×10^{13}				4.9×10^{15}	5.0×10^{16}	5.0×10^{17}	5.1×10^{18}
	$[V]$								
1700 °C	$E_\mathrm{F}-E_\mathrm{V}$ (eV)	0.72	1.09	1.26	1.28	1.29	1.31	1.48	1.84
1 atm H	$[\mathrm{H}_i]$	4.2×10^{17}	4.8×10^{16}	1.8×10^{16}	1.5×10^{16}	1.5×10^{16}	1.3×10^{16}	4.8×10^{15}	5.8×10^{14}
$\mu_\mathrm{H}=-15.75$ eV	$[V+n\mathrm{H}]$								1.2×10^{12}
	$[V]$	2.6×10^{15}	3.5×10^{13}	4.6×10^{12}	3.6×10^{12}	3.5×10^{12}	2.6×10^{12}		
1700 °C	$E_\mathrm{F}-E_\mathrm{V}$ (eV)	0.72	1.08	1.26	1.28	1.29	1.31	1.48	1.84
10 atm H_2	$[\mathrm{H}_i]$	2.7×10^{15}	3.2×10^{14}	1.1×10^{14}	1.0×10^{14}	1.0×10^{14}	8.3×10^{13}	3.0×10^{13}	3.7×10^{12}
$\mu_\mathrm{H}=-16.61$ eV	$[V+n\mathrm{H}]$								
	$[V]$	2.6×10^{15}	3.8×10^{13}	4.6×10^{12}	3.6×10^{12}	3.5×10^{12}	2.6×10^{12}		

detectable levels (especially in hexagonal material). Finally, note that hydrogen incorporation is primarily governed by the position of the Fermi level. The closer it is to the band edges, the more favorable are conditions for the charged hydrogen defects. Therefore, a decrease of temperature increases hydrogen incorporation during growth.

2. Hydrogen-plasma treatment

Plasma treatment is also a nonequilibrium process but, apart from the surface region, a stationary state between the concentration of atomic H ($\mathrm{H}^+ + e^-$) in the plasma and hydrogen in the crystal can be assumed. The concentrations of hydrogen defects in a stoichiometric 3*C*-SiC crystal in equilibrium with 0.03 atm H at 300 °C (typical temperature and pressure of H-plasma treatments) is shown in Table IV. Under such conditions Eq. (22) gives $\mu_\mathrm{H}=-13.84$ eV. As can be seen, the interstitial hydrogen incorporation in *p*-type samples equals the net carrier concentration while no significant amount of ($V_\mathrm{C}+n\mathrm{H}$) is created. On the contrary, ($V_\mathrm{Si}+n\mathrm{H}$) defects are dominant in *n*-type samples: quantities equal to half the net carrier concentration are created in 3*C*-SiC.

3. Annealing in hydrogen

In contrast to the above processes, in the case of annealing in H_2, the crystal is indeed in equilibrium with the ambient gas. The only successful experiment of this kind was carried out on 6*H*-SiC at $p=10$ atm between $T=1400$ and 1700 °C.[7] Table IV contains concentrations calculated in stoichiometric 3*C*-SiC assuming equilibrium with 10 atm H_2 at $T=1700$ °C. At this temperature 10% of hydrogen is assumed to be atomic, so data are also given for equilibrium with 1 atm H. (The corresponding μ_H values are -16.61 eV for H_2 and -15.75 eV for H.) Here, the concentration of atomic (positive) H is still significant in highly doped *n*-type samples as well. Again, the atomic hydrogen content of the gas is more effective. The concentration of atomic interstitial hydrogen in highly doped *p*-type samples is somewhat lower than in the case of the plasma treatment. In contrast, in *n*-type material, the concentration of ($V_\mathrm{Si}+n\mathrm{H}$) defects is low. (The latter may reach detectable levels in hexagonal polytypes.)

4. Implantation

Implantation can obviously create almost any nonequilibrium concentration of hydrogen along with intrinsic defects. The relative stabilities per hydrogen atom and the binding energies of H and H_2 in vacancies, as given in Eqs. (1)–(8), can serve as a guide to the complexes arising in the postannealing process. It is interesting to note that, unlike in Si, H^+ is the most stable interstitial form in *p*-type and intrinsic 3*C*-SiC. In *n*-type material, however, H_2 is more stable than H^-. This could explain the observation that hydrogen diffuses considerably more slowly in *n*-type than in *p*-type samples.[19] It has to be noted, however, that diffusion after implantation should be limited primarily by trapping in silicon vacancies [cf. Eqs. (1) and (6)]. Our calculated binding energies between V_Si and H are within the bounds deduced from experiments.[17,18]

B. The effect of hydrogen on carrier concentration in SiC

Hydrogen is best known in semiconductor technology for passivating carrier traps arising due to the dangling bonds in amorphous silicon solar cells. This kind of passivation is meant both in the chemical and the electrical sense: atomic hydrogen reacts with the free valence of a silicon atom, establishing a chemical bond. The bonding combination of the silicon sp^3 hybrid with the hydrogen s orbital becomes doubly occupied and is pushed into the valence band, while the antibonding combination is empty and is shifted into the conduction band. As a consequence no electrically active state remains, i.e., in the usual formulation the carrier trap con-

nected with the dangling bond is removed from the gap. In crystalline semiconductors the most important intrinsic carrier traps are vacancies. Hydrogen passivates the vacancy in crystalline silicon and (see Sec. III C) the silicon vacancy in 3*C*-SiC as well. The effectiveness of hydrogen passivation of traps depends on the way hydrogen is introduced. High temperature plasma anneals may create ($V_{Si}+n$H) electron traps ($n<4$) in *n*-type hexagonal samples, instead of passivating the existing V_{Si} ones. In contrast to the case of V_{Si}, the carbon vacancy in SiC (in both cubic and hexagonal forms; see Sec. III D) can be passivated by hydrogen in the chemical sense only, but the hole trap behavior remains because of hydrogen entering three-center bonds between two silicon atoms, instead of saturating one dangling bond. Hydrogen can passivate dopants as well, forming complexes in which no free valence remains. (H is not necessarily bonded to the dopant.) Alternatively, the electrical activity of hydrogen defects (away from the dopant) may compensate that of the dopant. In Sec. III A we have shown that interstitial hydrogen is a shallow donor in 3*C*-SiC, more abundant in *p*-type material. Therefore, compensation of acceptors is expected there. In hexagonal material H_i is likely to be an amphoteric carrier trap, since we predict the $(+/-)$ occupation level at around $E_V+2.4$ eV, i.e., farther away from the CB. Comparing the $(+/0)$ occupation level at $E_V+2.3$ in 3*C*-SiC (or the $+/-$ occupation level expected at around $E_V+2.4$ in hexagonal polytypes) with that of the shallow dopants (Fig. 4), the formation of acceptor-hydrogen complexes is strongly favored because of the Coulomb attraction of the oppositely charged centers. The formation of (Al-H) complexes has been reported in *p*-type material.[12] No such attraction occurs between H and the shallow donors in 3*C*-SiC. However, regarding the $(+/-)$ occupation level of H_i, as quoted above, and the higher lying $(+/0)$ level of the shallow donors, we expect attraction in hexagonal material. Still, due to the low abundance of interstitial hydrogen in *n*-type as-grown or plasma-treated SiC, neither passivation by complex formation nor compensation of donors can be expected in 3*C*-SiC. In *n*-type hexagonal polytypes, where donor + hydrogen complexes may form due to their mutual attraction, high temperature H_2 annealing can create obervable concentrations (see the H_i concentrations shown in Table IV), although we expect them to be at least an order of magnitude lower than those of the acceptor-hydrogen complexes in *p*-type samples. The main effect of hydrogen in *n*-type samples is the formation of ($V_{Si}+n$H) electron traps. Exposure of *n*-type material (especially hexagonal polytypes) to atomic hydrogen, therefore, may result in a decrease of the *n*-type carrier concentration. The presence of hydrogen in *p*-type hexagonal material after low temperature hydrogen-plasma treatment has been confirmed through its passivating effect.[9,10] At a doping level of 7×10^{17} cm^{-3} the passivation was much more prevalent in *p*-type than in *n*-type samples after a low temperature ECR plasma treatment.[10] dc plasma treatment in the same doping range [$(0.2–3)\times10^{18}$ cm^{-3}] but at higher temperature (300–700 °C) showed a free carrier decrease in *n*-type material due to intrinsic defect formation.[14] These findings seem to be qualitatively consistent with the discussion here, and the predictions of Table IV. In CVD-grown epitaxial SiC layers hydrogen may have a fourth way of influencing the carrier concentration (in addition to dopant passivation or compensation and carrier trapping). Doping in this case is realized in growth based on the site competition mechanism.[4] By tuning the C/Si ratio, the access of N to C sites or of B to Si sites is facilitated. Obviously, if hydrogen is present, there is one more possibility and H may fill the vacancies before the dopants get there. As shown above, hydrogen incorporation is substantial only in *p*-type samples, so the formation energy of B_{Si} and of ($V_{Si}+4$H) should be compared. Therefore, we have calculated the total energy of a 32-atom SCM containing boron in the substitutional position on the Si site. Under C-rich conditions and assuming the limit of the boron chemical potential to be equal to that in a boron crystal,[66] the formation energy of neutral B_{Si} is 0.27 eV. (Note that this is only a rough estimate, for the 32-atom unit is definitely too small for a shallow acceptor.) Estimating also the formation energy of neutral ($V_{Si}+4$H) from the available data (see the discussion about CVD epilayers in Sec. IV A) gives a value very much higher than this, so hydrogen does not hinder boron incorporation. During the annealing process after boron implantation, however, B_i and H_i compete for the existing V_{Si} defects. Using Eqs. (1) and (4), the energy gain of the reaction

$$V_{Si}+4H_i\rightarrow(V_{Si}+4H) \tag{26}$$

can be estimated to be 8.4 eV, while the gain of the reaction

$$V_{Si}+B_i\rightarrow B_{Si} \tag{27}$$

is only about 7.9 eV.[34] Therefore, hydrogen may restrict the activation efficiency of the implanted boron. Work in this direction is in progress.

C. Detection of hydrogen-related defects in SiC

1. Vibrational spectroscopy

The only unambiguous signature of hydrogen in SiC comes from PL experiments,[15,16] where the phonon replicas were assumed to arise from the local C-H modes in ($V_{Si}+$H). The stretching mode frequency we calculated in 3*C*-SiC, 2961 cm^{-1}, is well within the range measured in 6*H*-SiC (2962,2977,2988 cm^{-1}) and in 4*H*-SiC (2959,2985 cm^{-1}). Our results also explain why these signals were seen only in *p*-type material and why no Si-H modes around 2100 cm^{-1} were observed. Since V_{Si} is negatively charged during the post implantation anneal for almost all practical levels of doping while V_C is positive in *p*-type material, H^+ will predominantly form ($V_{Si}+$H) complexes. [The binding energy is also higher in ($V_{Si}+$H) than in (V_C+H).] However, the equlibrium concentration of hydrogen is very low in *n*-type material. (In strongly *n*-type hexagonal samples H_i is negative and will be repelled by both vacancies.) The presence of (V_C+H) defects can only be expected in *p*-type CVD epilayers grown under Si-rich conditions or in plasma-treated samples. Even there, the Si-H stretching modes will be far outside the 2100–2300 cm^{-1} range expected, as explained in Sec. III D.

2. Paramagnetic resonance

The present study does not allow us to elaborate on the quantitative aspects of hydrogen-related paramagnetic centers, but we would like to comment on the detectable ones and their symmetry.

We do not expect a readily detectable EPR signal from interstitial H in 3*C*-SiC, partly because of the low relative stability of the neutral charge state (Sec. III A), but more importantly because of the many possible ways a neutral interstitial H can get trapped at other defects. Paramagnetic states of the $(V+n\mathrm{H})$ defects should be observable in *p*-type CVD epilayers after electron irradiation and heat treatment (see Table III). Still, no paramagnetic H-related defect has yet been reported, even though V_{Si} (Refs. 46 and 67–69) and V_{C} (Ref. 70) appear to be easily seen in all polytypes by EPR or optically detected magnetic resonance (ODMR). Among the $(V_{\mathrm{C}}+\mathrm{H})$ complexes $(V_{\mathrm{C}}+\mathrm{H})^0$, $(V_{\mathrm{C}}+\mathrm{H})^{2+}$, and $(V_{\mathrm{C}}+2\mathrm{H})^+$ are paramagnetic. The latter is marginally unstable in equilibrium, similar to V_{C}^+, but may have a considerable lifetime under nonequilibrium conditions. The $(V_{\mathrm{C}}+\mathrm{H})$ system is bistable (i.e., the $3+$ charge state has a different configuration from that of the $1+$ and neutral charge states), and thus we do not expect $(V_{\mathrm{C}}+\mathrm{H})^{2+}$ to manifest itself. We note that practical measurements are carried out mostly under nonequilibrium conditions, unless the sample is cooled down very slowly in the dark. As mentioned in Sec. III D, V_{C}^+ and $(V_{\mathrm{C}}+2\mathrm{H})^+$ have very similar spin distributions (Fig. 12). However, in 3*C*-SiC V_{C}^+ has D_{2d} while $(V_{\mathrm{C}}+2\mathrm{H})^+$ has D_2 symmetry.

An observed EPR center ($T5$) with D_2 symmetry was assigned to V_{C}^+ in electron irradiated CVD layers of 3*C*-SiC by Itoh *et al.*[70,71] This assignment is rather curious, since a positively charged vacancy should undergo a D_{2d} rather than a D_2 distortion.[72] This is also what the present and other[39] calculations find. The $T5$ center has only been observed in *p*-type and not even in weakly *n*-type 3*C*-SiC. Itoh *et al.* explain this by assuming that the $(+/0)$ occupation level is at midgap, and the defect is not in the paramagnetic state in *n*-type samples. This explanation also contradicts theory. First, V_{C} is a negative *U* system, so V_{C}^+ could only be observed under nonequilibrium conditions (e.g., in light), but then it could be observed in *n*-type samples as well. Second, calculations unequivocally predict V_{C} to have a donor level well in the upper half of the gap. Assigning the $T5$ center to $(V_{\mathrm{C}}+2\mathrm{H})^+$ instead would allow a more consistent interpretation of the results. This complex does have D_2 symmetry, and it can be formed during electron irradiation if there is a sufficient amount of interstitial hydrogen in the as-grown epilayers. As can be seen from Table III, the detection limit of the concentration of mobile, interstitial hydrogen should occur when the Fermi level is somewhere below midgap. Therefore, H-related defects, such as $(V_{\mathrm{C}}+2\mathrm{H})$ can only be observed in *p*-type samples and not even in weakly *n*-type samples. The $T5$ center anneals out around 200 °C with an activation energy of 1.45 eV. This was interpreted by Itoh *et al.* as the activation energy of V_{C} diffusion. We may assume that this is indeed the case, and still assign the $T5$ signal to $(V_{\mathrm{C}}+2\mathrm{H})$. Then, however, the disappearance of the $T5$ signal should be connected to the reactions given by Eq. (10), i.e., to the redistribution of hydrogen in the vacancies. An alternative could be the decomposition of the $(V_{\mathrm{C}}+2\mathrm{H})$ complex into $(V_{\mathrm{C}}+\mathrm{H})$ as in Eq. (8). It is difficult to tell where the Fermi level is after electron irradiation. Assuming an energy balance of 1.45 eV in Eqs. (8) and (9) gives $E_{\mathrm{F}}-E_{\mathrm{V}}=0.7$ eV, which is not unreasonable.

Based on symmetry and spin distribution, it is also possible that the EI1 center, which has been seen only in *p*-type hexagonal material,[73] could be assigned to $(V_{\mathrm{C}}+\mathrm{H})^0$. It should be noted that the EI1 and $T5$ centers are very similar in *g* value, the strength of the hyperfine interaction with the nearest Si neighbors, and the annealing behavior. The electronic structure of the EI5 center in 4*H*- and 6*H*-SiC, which was recently identified by ESR as V_{C}^+,[74] is, however, very different from that of the $T5$ center:[70,71] in the case of the EI5 center, the hyperfine interaction with the nearest Si neighbors is about two times larger than that of the $T5$ center. The EI5 center is also stable at higher temperatures as compared to the $T5$ center (the EI5 center is observed after electron irradiation at 400 °C). As mentioned in Sec. III D, $(V_{\mathrm{C}}+\mathrm{H})^0$ and V_{C}^- both have C_{2v} symmetry and very similar spin distribution (see Fig. 10). Annealing around 200 °C removes the EI1 center, together with the EI3 ($S=1$) center [cf. Eq. (6)]. At the same time two new, similar spectra appear.[74] It is conceivable that EI1 and EI3 correspond to $(V_{\mathrm{C}}+\mathrm{H})^0$ and the triplet charge state of $(V_{\mathrm{C}}+2\mathrm{H})^0$ observed under nonequilibrium conditions: their disappearance is connected with their dissociation—and the possible appearance of the true V_{C} signals.

We note that an $S=1$ center with C_{3v} symmetry was found[75] using ODMR in 3*C*-SiC and assigned to a complex of V_{Si} with another defect. It is tempting to identify this defect with the triplet state of $(V_{\mathrm{Si}}+\mathrm{H})^-$, assuming that the wet etching applied to remove the Si substrate introduced hydrogen in addition to the amount grown in during epitaxial growth.

3. Deep level transient spectroscopy

To the best of our knowledge, the only DLTS study related to hydrogen was carried out in 6*H*-SiC epilayers grown by CVD and doped *n*-type to 10^{15}–10^{16} cm^{-3}.[20] The samples were first irradiated by electrons, then by deuterium, and finally annealed at 800 °C. After electron irradiation acceptor levels at $E_{\mathrm{C}}-0.34/0.41$ eV (the two values were assigned to inequivalent lattice sites) and at $E_{\mathrm{C}}-0.62/0.64$ eV as well as a donor level at $E_{\mathrm{C}}-0.51$ eV were found. After deuterium implantation, the $E_{\mathrm{C}}-0.34/0.41$ eV peak disappeared but no new peak arose. The following heat treatment restored the $E_{\mathrm{C}}-0.34/0.41$ eV peak but eliminated the one at $E_{\mathrm{C}}-0.51$ eV and greatly reduced (and shifted) the one at $E_{\mathrm{C}}-0.62/0.64$ eV. A series of isochronal anneals showed that the $E_{\mathrm{C}}-0.51$ eV peak anneals out around 200 °C with an activation energy identical with that of the $T5$ center in 3*C*-SiC (see Sec. IV A 2). At the same time a new defect appeared with a peak at $E_{\mathrm{C}}-0.87$ eV. Based on

the very similar annealing characteristics to the $T5$ center, the $E_C-0.51$ eV peak was assigned[20] to the donor level of V_C.

Assigning the $T5$ center to (V_C+2H) would then imply that the $E_C-0.51$ eV peak is also connected with a (V_C+nH) complex. The in-grown H content of the epilayers could have been in the 10^{14} cm^{-3} range in the as-grown samples of Ref. 20, but the (V_C+nH) concentration must have been very low (see Table III). Electron irradiation may have increased the concentration of vacancies, and could have increased the concentration of vacancy + hydrogen complexes as well, since irradiation increases the temperature and can cause diffusion. Of course, the increase in (V_C+nH) concentration is limited by the availability (the original concentration) of H. That explains the observed low sensitivity of the $E_C-0.51$ eV peak to the electron dose. If the dominant (V_C+nH) defect is already present in the spectrum, further hydrogen implantation obviously does not introduce a new peak and the low dose (10^{11} cm^{-2}) probably could not have caused a significant increase in peak height. Unfortunately, the calculated $(2+/0)$ occupation level of (V_C+2H) is at $E_V+1.8$ eV in $3C$-SiC. Since the defect orbitals are rather well localized, we do not expect a significant difference in $6H$-SiC, with respect to the valence band. Therefore, our estimate in $6H$-SiC is around $E_C-1.3$ eV, which is substantially too low compared to the observed peak position. In fact, we cannot predict any donor level as high as this for any of the carbon vacancy related defects. For V_C we obtain the $(2+/0)$ occupation level at $E_V+1.93$ eV (or at $E_V+1.55$ eV if no LDA gap correction is applied). Zywietz *et al.* have reported the occupation levels of V_C in $3C$- and $4H$-SiC (without gap correction).[39] Their values, $E_V+1.56$ eV and $E_V+1.54$ eV, respectively, show that theory cannot identify the $E_C-0.51$ eV DLTS peak in $6H$-SiC with the donor state of a carbon vacancy either. Further work in this direction is necessary.

V. SUMMARY

Based on *ab initio* LDA calculations in 32- and 128-atom supercells of $3C$-SiC, we have established the stable configurations of hydrogen and dihydrogen defects. The calculated formation energies were used to give semiquantitative estimates for their concentrations after CVD growth, low temperature H-plasma anneal, or heat treatment in high temperature hydrogen gas. Thermochemistry between interstitial hydrogen and vacancies, introduced by implantation, is also discussed. We have found that interstitial H is readily incorporated in *p*-type material during growth, and it acts as a shallow donor in $3C$-SiC, compensating the acceptors. Complex formation with the latter is also likely. In *n*-type material interstitial H_2 is the more stable form but the formation energy is too high to allow for significant incorporation. (V_C+H) behaves as a hole trap, whereas $(V_{Si}+H)$ is an electron trap. The former has a lower formation energy, but if both types of vacancy are present implanted hydrogen is preferentially trapped by V_{Si}. The electron trap V_{Si} can be passivated by four hydrogen atoms but V_C can accommodate only two and thereby remains a hole trap. Plasma treatment introduces a sufficient amount of interstitial hydrogen for complete passivation in *p*-type material. In *n*-type material, the dominant defects are $(V_{Si}+nH)$ electron traps, in sufficient amount to halve the free carrier concentration. High temperature annealing is effective in introducing hydrogen even to *n*-type material. We have also calculated vibrational frequencies, spin distributions, and occupation levels in order to facilitate spectroscopic identification of these defects. We suggest that some of the paramagnetic signals assigned earlier to pure vacancies might originate from $(V+nH)$ complexes. Qualitative extrapolation of our results to hexagonal polytypes explains the observed effects of hydrogen on the free carrier concentration. Calculations for the $4H$ polytype are in progress.

ACKNOWLEDGMENTS

The authors are indebted to P. R. Briddon for his parallel version of the supercell AIMPRO code. Helpful discussions with R. P. Devaty are appreciated. Support from the Hungarian OTKA Grants No. T-22139, No. T32174, and No. FKFP 0289/97 as well as from the bilateral programs between Hungary and the U.S. (JF Grant No. 667), Sweden (IVA-MTA Grant No. 36), and South Africa (Grant No. DAK 7/98) is appreciated. This work was also supported by grants from the Pittsburgh Supercomputer Center (PHY970006P) and the Swedish National Supercomputer Center (2000018).

[1] *Hydrogen in Semiconductors*, Vol. 34 of *Semiconductor and Semimetals*, edited by J.I. Pankove and N.M. Johnson (Academic Press, New York, 1991).

[2] *Defects in Silicon: Hydrogen*, edited by J. Weber and A. Mesli, special issue of Mater. Sci. Eng., B **58** (1999).

[3] *Proceedings of the 20th International Conference on Defects in Semiconductors, ICDS-20*, edited by C.G. Van de Walle and W. Walukiewicz [Physica B **273-274** (1999)].

[4] D.J. Larkin, P.G. Neudeck, J.A. Powell, and L.G. Matus, Appl. Phys. Lett. **65**, 1659 (1994).

[5] D.J. Larkin, S.G. Sridhara, R.P. Devaty, and W.J. Choyke, J. Electron. Mater. **24**, 289 (1995).

[6] D.J. Larkin, Phys. Status Solidi B **202**, 305 (1997).

[7] F. Gendron, L.M. Porter, C. Porte, and E. Bringuier, Appl. Phys. Lett. **67**, 1253 (1995).

[8] B. Clerjaud, F. Gendron, C. Porte, and W. Wilkening, Solid State Commun. **93**, 463 (1995).

[9] G.J. Gerardi, E.H. Pointdexter, and D.J. Keeble, Appl. Spectrosc. **50**, 1428 (1996).

[10] G. McDaniel, J.W. Lee, E.S. Lambers, S.J. Pearton, P.H. Holloway, F. Ren, J.M. Grow, M. Bashkaran, and R.G. Wilson, J. Vac. Sci. Technol. A **15**, 885 (1997).

[11] N. Achtziger, J. Grillenberger, W. Witthuhn, M.K. Linnarsson, M. Janson, and B.G. Svensson, Appl. Phys. Lett. **73**, 945 (1998).

[12] C. Hülsen, N. Achtziger, U. Reislöhner, and W. Witthuhn, in *ICSCRM'99*, edited by C.H. Carter, R.P. Devaty, and G.S. Rohrer [Mater. Sci. Forum **338-342**, 929 (2000)].
[13] T.E. Tiwald, J.A. Woollam, S. Zollner, J. Christiansen, R.B. Gregory, T. Wetteroth, S.R. Wilson, and A.R. Powell, Phys. Rev. B **60**, 11 464 (1999).
[14] A.O. Konstantinov, N.S. Konstantinova, O.I. Kon'kov, E.I. Terukov, and P.A. Ivanov, Fiz. Tekh. Poluprovodn. [Semiconductors **28**, 209 (1994)].
[15] W.J. Choyke and L. Patrick, Phys. Rev. Lett. **29**, 355 (1972).
[16] W.J. Choyke and L. Patrick, Phys. Rev. B **9**, 3214 (1974).
[17] M.K. Linnarsson, J.P. Doyle, and B.G. Svensson, in *III-Nitride, SiC, and Diamond Materials for Electronic Devices*, edited by D.K. Gaskill, C.D. Brandt, and R.J. Nemanich, Mater. Res. Soc. Symp. Proc. No. **423** (Materials Research Society, Pittsburgh, 1996), p. 625.
[18] M. Janson, M.K. Linnarsson, A. Hallén, and B.G. Svensson, in *Hydrogen in Semiconductors and Metals*, edited by N.H. Nickel, W.B. Jackson, and R.C. Bowman, Mater. Res. Soc. Symp. Proc. No. **513** (Materials Research Society, Pittsburgh, 1998), p. 439.
[19] M. Janson, M.S. thesis, Royal Institute of Technology, Stockholm, 1998.
[20] M.O. Aboelfotoh and J.P. Doyle, Phys. Rev. B **59**, 10 823 (1999).
[21] S.K. Estreicher, Mater. Sci. Forum **148-149**, 349 (1994).
[22] C.H. Chu and S.K. Estreicher, Phys. Rev. B **42**, 9486 (1990).
[23] M.A. Roberson and S.K. Estreicher, Phys. Rev. B **44**, 10 578 (1991).
[24] L. Pavesi, P. Gianozzi, and F.K. Reinhart, Phys. Rev. B **42**, 1864 (1990).
[25] T.L. Estle, S. Estreicher, and D.S. Marinick, Hyperfine Interact. **32**, 637 (1987).
[26] S. Estreicher, Phys. Rev. B **36**, 9122 (1987).
[27] P. Deák, L.C. Snyder, and J.W. Corbett, Phys. Rev. B **37**, 6887 (1988).
[28] C.G. Van de Walle, Y. Bar-Yam, and S.T. Pantelides, Phys. Rev. Lett. **60**, 2761 (1988).
[29] A. Gali, B. Aradi, P. Deák, W.J. Choyke, and N.T. Son, Phys. Rev. Lett. **84**, 4926 (2000).
[30] P. Deák, A. Gali, B. Aradi, N.T. Son, E. Janzén, and W.J. Choyke, *ICSCRM'99* (Ref. 12), p. 817.
[31] W. Kohn and L.J. Sham, Phys. Rev. **140**, A1133 (1965).
[32] M. Bockstede, A. Kley, J. Neugebauer, and M. Scheffler, Comput. Phys. Commun. **107**, 187 (1997).
[33] N. Troullier and J.L. Martins, Phys. Rev. B **43**, 1993 (1991).
[34] M. Bockstedte (private communication).
[35] G.A. Baraff and M. Schlüter, Phys. Rev. B **30**, 1853 (1984).
[36] H.J. Monkhorst and J.K. Pack, Phys. Rev. B **13**, 5188 (1976).
[37] S.G. Louie, M. Schlüter, J.R. Chelikowski, and M.L. Cohen, Phys. Rev. B **13**, 1654 (1976).
[38] A. Zywietz, J. Furthmüller, and F. Bechstedt, Phys. Status Solidi B **210**, 13 (1998).
[39] A. Zywietz, J. Furthmüller, and F. Bechstedt, Phys. Rev. B **59**, 15 168 (1999).
[40] The one-electron levels have not been corrected for spin polarization.
[41] C.G. Van de Walle, P.J.H. Denteneer, Y. Bar-Yam, and S.T. Pantelides, Phys. Rev. B **39**, 10 791 (1989).
[42] For charged defects the supercell LDA calculations introduce an artificial energy lowering interaction between the supercells, which is expected to be partially compensated by the error due to the neglect of long range relaxation for singly and doubly charged systems. See G. Makov and M.C. Payne, Phys. Rev. B **51**, 4014 (1995).
[43] R. Jones, Philos. Trans. R. Soc. London, Ser. A **341**, 351 (1992).
[44] G.B. Bachelet, D.R. Hamann, and M. Schlüter, Phys. Rev. B **26**, 4199 (1982).
[45] H_2 vibrations are atypical because the very small reduced mass ''amplifies'' the error in the calculated force constant.
[46] T. Wimbauer, B. Meyer, A. Hofstätter, A. Scharmann, and H. Overhof, Phys. Rev. B **56**, 7384 (1997).
[47] Breathing (pairing) mode distortion is the displacement of the first neighbors along [111] ($[\bar{1}\,\bar{2}2]$) given as a percentage of the calculated interatomic distances of the perfect lattice.
[48] F.P. Larkins and A.M. Stoneham, J. Phys. C **3**, L112 (1970).
[49] P. Deák, J. Miró, A. Gali, L. Udvardi, and H. Overhof, Appl. Phys. Lett. **75**, 2103 (1999).
[50] These occupation levels were predicted to be $E_V+0.56$ and $E_V+1.22$ eV by L. Torpo, R.M. Nieminen, K.E. Laasonen, and S. Pöykkö, Appl. Phys. Lett. **74**, 221 (1999), and $E_V+1.11$ and $E_V+1.94$ eV in Ref. 39. In the former case, no LDA gap correction was applied, while a full shift (equivalent to that of the extended states) was used in the latter. Our results contain a gap correction corresponding to 0.2 times the shift applied for extended states.
[51] a',a'' refer to the actual C_{1h} and a_1,e to the approximate C_{3v} symmetry.
[52] The values given in Eqs. (2)–(4) are from Gaussian-based calculations in a large MCM without zero point energy (ZPE) correction. The plane wave supercell calculation with ZPE correction gives 0.23 eV in Eq. (2).
[53] The statement about complete passivation by two hydrogen atoms in Ref. 30 was meant for the hyperdeep donor activity. (A donor level in the lower half of the gap is called hyperdeep. It is actually a hole trap.)
[54] Note that the $E_V+(2.1–2.3)$ eV given in Refs. 29 and 30 was in error. Correcting that and using -0.1 eV for the spin-polarization error gives $E_V+2.39$ eV.
[55] P. Deák, L.C. Snyder, M. Heinrich, C.R. Ortiz, and J.W. Corbett, Physica B **170**, 253 (1991).
[56] B. Bech Nielsen, P. Johannesen, P. Stallinga, and K. Bonde, Phys. Rev. Lett. **79**, 1507 (1997).
[57] C. Van de Walle, Phys. Rev. B **49**, 4579 (1994).
[58] Note that this definition differs from that used in Ref. 39 by a factor of 0.5.
[59] O. Kubaschewski and C.B. Alcock, *Metallurgical Thermochemistry* (Pergamon, Oxford, 1979).
[60] The zero point energy was calculated from the stretching modes including the H atoms and their immediate neighbors, namely, these are the ones that change between various configurations. (The contribution of the bending modes is small.)
[61] J.E. Northrup, R.D. Felice, and J. Neugebauer, Phys. Rev. B **56**, R4325 (1997).
[62] The deviation of the calculated E(H) from 1 Ry is mainly due to the self-interaction error of the LDA method.
[63] S.M. Sze, *Physics of Semiconductor Devices* (Wiley-Interscience, New York, 1969).
[64] R. Kaplan, R.J. Wagner, H.J. Kim, and R.F. Davies, Solid State Commun. **55**, 67 (1985).

[65] C. Persson and U. Lindefelt, J. Appl. Phys. **82**, 5496 (1997).
[66] The limit to ''boron-rich'' conditions in the gas phase is when crystalline boron is formed instead of B entering the SiC crystal.
[67] H. Itoh, M. Yoshikawa, I. Nashiyama, S. Misawa, H. Okumura, and S. Yoshida, IEEE Trans. Nucl. Sci. **NS-37**, 1732 (1990).
[68] J. Schneider and K. Maier, Physica B **185**, 199 (1993).
[69] E. Sörman, N.T. Son, W.M. Chen, O. Kordina, C. Hallin, and E. Janzén, Phys. Rev. B **61**, 2613 (2000).
[70] H. Itoh, M. Yoshikawa, I. Nashiyama, S. Misawa, H. Okumura, and S. Yoshida, J. Electron. Mater. **21**, 707 (1992).
[71] H. Itoh, A. Kawasubo, T. Ohshima, M. Yoshikawa, I. Nashiyama, S. Tanigawa, S. Misawa, H. Okumura, and S. Yoshida, Phys. Status Solidi A **162**, 173 (1997).
[72] G.D. Watkins, in *Deep Centers in Semiconductors*, edited by S.T. Pantelides (Gordon and Breach, New York, 1986), p. 147.
[73] N.T. Son, W.M. Chen, J.L. Lindström, B. Monemar, and E. Janzén, Mater. Sci. Eng., B **61-62**, 202 (1999).
[74] N.T. Son, P.N. Hai, and E. Janzén, in *ECSCRM200*, edited by G. Pensl, D. Stephani, and M. Hundhausen, Mater. Sci. Forum **353-356**, 499 (2001).
[75] N.T. Son, E. Sörman, W.M. Chen, C. Hallin, O. Kordina, B. Monemar, and E. Janzén, Phys. Rev. B **55**, 2863 (1997).